[redacted]

NASA TECHNICAL MEMORANDUM

NASA TM X-976

(NASA-TM-X-976) EFFECTS OF CONFIGURATION GEOMETRY ON THE TRANSONIC AERODYNAMIC CHARACTERISTICS OF A SIMULATED LAUNCH VEHICLE T.C. Kelly, et al (NASA) Jul. 1964 43 p

N72-73345

Unclas

00/99 32186

X64 15569

Code 2

cat 30

43p

NASA TM X-976

CLASSIFICATION CHANGED

UNCLASSIFIED

TO

By Authority of TD-72-235 Date 6-8-72

EFFECTS OF CONFIGURATION GEOMETRY ON THE TRANSONIC AERODYNAMIC CHARACTERISTICS OF A SIMULATED LAUNCH VEHICLE

by Thomas C. Kelly and Thomas P. Ross

Langley Research Center
Langley Station, Hampton, Va.

NATIONAL AERONAUTICS AND SPACE ADMINISTRATION • WASHINGTON, D. C. • JULY 1964

[redacted]

[redacted]

EFFECTS OF CONFIGURATION GEOMETRY ON THE TRANSONIC AERODYNAMIC CHARACTERISTICS OF A SIMULATED LAUNCH VEHICLE

By Thomas C. Kelly and Thomas P. Ross

Langley Research Center
Langley Station, Hampton, Va.

GROUP 4
Downgraded at 3 year intervals;
declassified after 12 years

[redacted]FIED

[redacted]aterial contains information [redacted]he [redacted]of the U[redacted] the meaning o[redacted]itle 18, U.S.C., Secs. 79[redacted]velation [redacted]any manner to an unau[redacted]son [redacted]ohibited by law.

NATIONAL AERONAUTICS AND SPACE ADMINISTRATION

[redacted]

[redacted]

EFFECTS OF CONFIGURATION GEOMETRY ON THE TRANSONIC AERODYNAMIC CHARACTERISTICS OF A SIMULATED LAUNCH VEHICLE*

By Thomas C. Kelly and Thomas P. Ross
Langley Research Center

SUMMARY

15569

An investigation to determine the effects of nose-cone angle and bluntness, upper-stage fineness ratio, and stage transition flare angle on the aerodynamic characteristics of a simulated launch vehicle was conducted at Mach numbers from 0.40 to 1.20, angles of attack from about -4° to 18°, and at test Reynolds numbers per foot on the order of 3.7×10^{6}.

The results indicate that increases in nose-cone angle had only slight effects on normal-force, pitching-moment, and center-of-pressure characteristics, but caused a near-linear increase in forebody axial force with increasing nose angle at Mach numbers above 0.40. Increasing the nose bluntness had no noticeable effect on axial force at an angle of attack of 0° over the Mach number range investigated.

At low angles of attack, increases in upper-stage fineness ratio, although exhibiting little effect on normal-force-curve slope, caused increases in pitching-moment-curve slope and forward shifts in center-of-pressure location which remained fairly constant over the Mach number range investigated.

Increasing the stage transition flare angle had little effect on the aerodynamic characteristics other than axial force. For the highest flare angle investigated, increases in axial-force coefficient with increases in angle of attack up to 10° occurred at a Mach number of 1.2, as a probable result of variations in flow separation with angle of attack for this configuration. Conf. author

INTRODUCTION

The complex nature of the flow in the transonic speed range has precluded the development of theoretical methods which may be used to predict launch-vehicle aerodynamic characteristics accurately. Furthermore, the available experimental information has not permitted the development of reliable empirical methods of prediction. As a result, wind-tunnel investigations are generally required to determine the transonic characteristics of proposed launch

---

*Title, Unclassified.

[redacted]

vehicles and also to determine effects of modifications to existing launch vehicles. Although experimental results are available for a number of specific vehicles (e.g., refs. 1 to 3) and for systematic variations of relatively low-fineness-ratio single-stage configurations (e.g., refs. 4 to 6), investigations of a systematic nature for multistage configurations, which would aid in the development of the empirical methods noted earlier, have generally either been conducted at supersonic speeds or have been involved with the development of a particular launch vehicle (e.g., refs. 7 and 8).

The present investigation was undertaken as an adjunct to the aerodynamic loads investigation of reference 9 in order to determine the effects of configuration geometry on the transonic aerodynamic force and moment characteristics of a simulated launch vehicle.

The investigation was conducted in the Langley 8-foot transonic pressure tunnel at Mach numbers from 0.40 to 1.20 and angles of attack from about -4° to 18°. The average test Reynolds number per foot was on the order of 3.7×10^{6}.

SYMBOLS

Aerodynamic force and moment data are referred to the body system of axes, with coefficients based on the maximum body cross-sectional area of 0.0524 square foot and the maximum body diameter of 3.10 inches. Moments are measured about a point located on the body center line three reference diameters forward of the model base.

A	maximum body cross-sectional area, 0.0524 sq ft
C_A	axial-force coefficient, $\frac{\text{Axial force}}{qA}$
$C_{A,b}$	base axial-force coefficient, $\frac{\text{Base axial force}}{qA}$
C_m	pitching-moment coefficient, $\frac{\text{Pitching moment}}{qAd}$
C_{m_α}	pitching-moment-curve slope, $\frac{\partial C_m}{\partial \alpha}$, per deg
C_N	normal-force coefficient, $\frac{\text{Normal force}}{qA}$
C_{N_α}	normal-force-curve slope, $\frac{\partial C_N}{\partial \alpha}$, per deg

d	maximum body diameter, 3.10 in.
M	Mach number
q	free-stream dynamic pressure
R	Reynolds number per foot
r	radius of nose-cone hemispherical cap
r_b	radius of nose-cone base
x_{cp}	center-of-pressure location, maximum body diameters forward of model base
α	angle of attack of body center line, deg
δ_F	stage transition flare half-angle, deg
δ_N	nose-cone half-angle, deg

APPARATUS AND TESTS

Model

Details and design dimensions of the several model configurations investigated are presented in figure 1. Configurations are separated into the three general groups described in subsequent sections and are numbered according to the system utilized in reference 9. It should be noted here that, for the investigation of reference 9, configuration numbers were assigned according to a proposed testing sequence and therefore do not always follow an orderly progression as far as model geometric variations are concerned.

Nose variations.- Configurations used to determine effects of nose angle and bluntness, shown in figure 1(a), had an upper-stage fineness ratio of 4.85, and a transition flare half-angle of 5°. Three pointed nose cones having half-angles of 15.3°, 22.5°, and 30° (configurations 4, 3, and 5, respectively) were investigated. In addition, two other 22.5° half-angle, rounded nose cones which had ratios of nose cap radius to cone base radius of 0.30 (configuration 6) and 0.60 (configuration 7) were tested.

Upper-stage variations.- Three model configurations were employed to determine the effects of variations in upper-stage fineness ratio. (See fig. 1(b).) For these configurations, the nose cone and transition flare half-angles were 22.5° and 5°, respectively, and the upper-stage fineness ratio was varied from 1.42 (configuration 1) to 2.99 (configuration 2) and to 4.85 (configuration 3).

Transition flare variations.- Four configurations were used to determine the effects of variations in transition flare angle. Each had a

22.5° half-angle conical nose and the transition flare half-angles were 5°, 10°, 15°, and 29.9° for configurations 3, 10, 8, and 9, respectively. (See fig. 1(c).) As noted in reference 9, the variations in transition flare angle were accompanied by variations in the upper-stage fineness ratio and in model overall length. These variations, which in reference 9 resulted from an attempt to place pressure orifices immediately ahead of the flare leading edge, were duplicated for the configurations of the present investigation.

Model photographs are provided in figure 2.

Tests and Procedure

The investigation was conducted at a stagnation pressure approximately equal to atmospheric. With the exception of configurations 6 and 7 (blunt nose-cone configurations), which were tested through the Mach number range at an angle of attack of 0° only, all configurations were tested through an angle-of-attack range extending from about -4° to 18° at Mach numbers from 0.40 to 1.20. Average test Reynolds numbers per foot and dynamic pressures for the investigation are given in figure 3.

The investigation was conducted with a transition strip located at a point 0.25 inch rearward of the nose-cone—upper-stage juncture. The transition strip was 0.1 inch wide and was composed of No. 80 carborundum grains (nominal size 0.0083 inch) set in a plastic adhesive.

Corrections

Effects of subsonic boundary interference in the slotted test section are considered to be negligible, and no corrections for these effects have been applied. Also, no results are presented for supersonic Mach numbers at which boundary-reflected disturbances would be expected to affect the results.

Axial-force results contained herein have been adjusted to the assumed condition of free-stream static pressure acting at the model base.

Accuracy

Accuracies of the measured coefficients, based upon instrument calibration and data repeatability, are estimated generally to be within the following limits:

	M = 0.40	M = 1.20
C_N	±0.070	±0.017
C_A	±0.015	±0.004
$C_{A,b}$	±0.012	±0.003
C_m	±0.188	±0.045

Model angle of attack is estimated to be accurate within ±0.1°.

PRESENTATION OF RESULTS

The figures presenting results of this investigation are listed in the following table:

	Figure
Variation with angle of attack of normal-force characteristics	4
Variation with angle of attack of axial-force characteristics	5
Variation with angle of attack of base axial-force characteristics . . .	6
Variation with angle of attack of pitching-moment characteristics . . .	7
Variation with angle of attack of center-of-pressure characteristics	8
Summary of aerodynamic characteristics in pitch, $\alpha \approx 0^{\circ}$	9
Effect of nose-cone angle on axial-force characteristics	10

In order to facilitate presentation of the data, staggered scales have been used in some of the figures and care should be taken in selecting the proper zero axis for each curve. Flagged points which appear in the center-of-pressure results at an angle of attack of 0° in figure 8 represent computed values which were obtained by using $C_{m_{\alpha}}$ and $C_{N_{\alpha}}$ measured at an angle of attack of approximately 0°.

DISCUSSION

Effect of Nose-Cone Angle

Normal-force curves for the configurations having varying nose angles, given in figure 4(a), exhibit an increase in slope with increasing angle of attack. The effects on the normal-force-curve slope measured at an angle of attack of 0° (fig. 9(a)) of increasing nose-cone angle from 15.3° to 30° are seen to be slight. Results presented in references 4 and 10 show similar effects.

Effects of a variation in nose-cone angle on the axial-force characteristics, presented in figure 5(a), indicate that the increases in axial-force coefficient associated with increases in nose-cone angle remain essentially constant at each Mach number over the angle-of-attack range of the present investigation. The effects of Mach number on the axial-force characteristics for the varying nose-angle configurations are presented in figure 9(a) and show that for an angle of attack of 0° positive increments in axial-force coefficient resulting from increases in nose-cone angle generally increase at the higher Mach numbers, as would be expected. Base axial-force coefficients (fig. 6(a)) indicate little or no effect of nose angle.

An interesting comparison may be made between the axial-force results of the present investigation and those given in reference 4, if two assumptions are made. The first is that for the present investigation the variations in axial force discussed previously are associated solely with variations in

nose-cone axial force, and the second is that the blunted conical noses of reference 4 and the pointed conical noses of the present investigation may be compared directly. Concerning the first assumption, results given in reference 9 for configurations identical to those of the present investigation indicate that interference effects resulting from variations in nose-cone angle are restricted to the cylindrical portion of the model forward of the transition flare. As a result, variations in axial-force coefficient with variations in nose-cone angle for the present investigation would be associated only with the nose cone. With regard to the second assumption, results given in references 10, 11, and 12 and results of the present investigation to be discussed subsequently herein indicate that, at least up to the Mach number for the sharp cone shock attachment, the effects of nose bluntness are essentially negligible.

Results of the aforementioned comparison are shown in figure 10. In figure 10(a), axial-force coefficients, plotted for several Mach numbers as a function of nose half-angle, exhibit a near-linear increase with increasing nose angle for most of the Mach numbers above 0.40. Coefficients are referenced to the cone base area in each case. A summary of these results (fig. 10(b)) indicates reasonably good agreement in the slopes measured for the curves of figure 10(a).

Effects of a variation in nose-cone angle on the pitching-moment and center-of-pressure characteristics, shown in figures 7(a) and 8(a) and summarized in figure 9(a), are seen to be slight.

Effect of Nose Bluntness

The effects on axial force of varying the nose bluntness ratio, or the ratio of nose hemispherical cap radius to cone base radius (r/r_b), are given for the 22.5° half-angle nose cone at $\alpha = 0^\circ$ in figure 9(b). As indicated earlier, these results show negligible effects of blunting over the bluntness ratio and Mach number ranges investigated. Examination of the results presented in references 10 and 11 indicates that, for configurations which have lower effective nose-cone angles than those of the present investigation, nose blunting also has little or no effect up to Mach numbers slightly over 1.0. At higher Mach numbers ($1.0 < M < 1.4$), the configurations which have relatively low values of bluntness ratio ($r/r_b \approx 0.27$) again show negligible effects of bluntness; however, sizable increases in drag due to bluntness above a Mach number of 1.03 are noted in reference 11 for a configuration having a bluntness ratio of about 0.77.

The reasons for the negligible effects on drag of nose blunting, as stated for the supersonic case in reference 11, hold also for the subsonic and transonic ranges, as is shown by the results of reference 9. Briefly, the flow reaches stagnation pressure at the nose apex and then experiences an extremely rapid expansion over the hemispherical nose portion, reaching local pressures considerably below those which exist for the pointed nose cone at the same location forward of the cone-cylinder juncture. Rearward of the hemispherical nose cap, local pressures for the blunted cone approach those of the pointed, or unmodified, cone. As noted in reference 11, the effect of the relatively

higher pressures acting over the nose apex region of the blunted nose is opposed by the effect of relatively lower pressures acting over a larger area to the rear. For the configurations of the present investigation and those of the references indicated, these opposing forces result in no measurable differences in axial-force coefficient between the pointed and blunt nose configurations.

It should be noted that the configurations of reference 10 are composed of cones, cone frustums, and cylinders in combination, and those of reference 11 are ogive cylinders; however, it would be expected that the local pressure variations associated with nose blunting would have similar effects on drag both for the configurations discussed previously and those of the present investigation.

Effect of Upper-Stage Fineness Ratio

Although the effects of increasing upper-stage fineness ratio on the normal-force-curve slope measured at an angle of attack of 0° are negligible (fig. 9(c)), noticeable effects on normal-force coefficient do appear at the higher angles of attack. (See fig. 4(b).) It should be remembered, of course, that increases in upper-stage fineness ratio are accompanied by increases in projected planform area. (See fig. 1(b).)

Axial-force results (fig. 5(b)) show that increases in upper-stage fineness ratio are accompanied by increases in axial force, the increments remaining relatively constant through the angle-of-attack range at each Mach number. These increments in axial force associated with increasing fineness ratio are approximately equal to those which would be expected to result from the increase in friction drag as the upper-stage length, and therefore the wetted area is increased. Mach number effects, presented in figure 9(c), are seen to be slight. The results given in reference 9 indicate that at the highest test Mach number, the broadening of the negative pressure-coefficient peak associated with the nose cone results in a reduction in pressures over the forward region of the transition flare for the configuration with the lowest fineness ratio relative to the other two. Although these variations would be expected to reduce the axial force somewhat for this configuration, the results of figure 9(c) indicate little or no discernible effect.

Pitching-moment characteristics (fig. 7(b)) show notable increases in pitching moment at positive angles of attack with increases in upper-stage fineness ratio, which result primarily from a forward movement of the nose cone relative to the moment reference center.

Center-of-pressure results, given in figures 8(b) and 9(c), indicate that forward movements in center-of-pressure location resulting from the overall increase in stage fineness ratio are on the order of one body diameter, the increment remaining fairly constant over the Mach number range.

Effect of Transition Flare Angle

As noted in the model section, variations in stage transition flare angle were accompanied by variations in upper-stage fineness ratio and in model overall length. Based upon a consideration of the effects of fineness ratio previously discussed, however, the variations in fineness ratio with flare angle would be expected to have generally only slight effects, particularly on the normal-force and axial-force characteristics.

Results presented in figures 4(c) and 9(d) indicate that little or no effects occur on normal force at the lower angles of attack as stage transition flare half-angle is increased from 5° to 29.9°. Noticeable, but generally random, effects occur at angles of attack greater than about 8° up to a Mach number of 1.0. The effects of transition flare angle on axial-force characteristics are given in figures 5(c) and 9(d). Generally, increases in either transition flare angle or Mach number resulted in increases in axial force. At a Mach number of 0.6, and with the exception of the 29.9° flared configuration which has a noticeably higher axial force, the general level of axial-force coefficients is the same for the various flare-angle configurations. As Mach number is increased to 0.80 and 0.90, noticeable increases in form drag occur, respectively, for the 15° and 10° flare configurations relative to the 5° flare configuration (fig. 9(d)). At the highest test Mach number increases in angle of attack up to about 10° are accompanied by increases in axial force for the 29.9° flare configuration (fig. 5(c)). These variations are a probable result of a decrease in flare-induced separation with increasing angle of attack over the lower portion of the body which results in sizable increases in positive pressures over the lower half of the flare as angle of attack is increased to 10°. (See ref. 9.)

Pitching-moment results, given in figures 7(c) and 9(d), show little effect of flare angle at the lower angles of attack. At the higher angles of attack, noticeable effects occur, although not in an orderly progression with regard to the geometric variations. The results are undoubtedly affected to some degree by differences in nose location relative to the moment reference center for the various configurations, and effects of these differences should, of course, be considered in any application of these results. Center-of-pressure results (figs. 8(c) and 9(d)) generally show only slight effects of flare-angle variation.

CONCLUSIONS

Results of an investigation conducted at transonic speeds to determine the effects of systematic variations in geometry on the aerodynamic characteristics of a simulated launch vehicle have indicated the following:

1. Increases in nose-cone angle had only slight effects on normal-force, pitching-moment, and center-of-pressure characteristics, but caused a near-linear increase in forebody axial force with increasing nose angle at Mach numbers above 0.40. Increasing the nose-bluntness ratio from 0 to 0.60 for

a 22.5° half-angle nose cone had no noticeable effect on axial force at an angle of attack of 0° over the Mach number range investigated.

2. At low angles of attack, increases in upper-stage fineness ratio, although exhibiting little effect on normal-force-curve slope, caused increases in pitching-moment-curve slope and forward shifts in center-of-pressure location which remained fairly constant over the Mach number range investigated. At the higher angles of attack, increases in upper-stage fineness ratio were accompanied by noticeable increases in normal-force coefficient.

3. Increasing the stage transition flare angle had little effect on the aerodynamic characteristics other than axial force. For the highest flare angle investigated, increases in axial-force coefficient with increases in angle of attack up to 10° occurred at a Mach number of 1.2, as a probable result of variations in flow separation with angle of attack for this configuration.

Langley Research Center,
National Aeronautics and Space Administration,
Langley Station, Hampton, Va., February 29, 1964.

REFERENCES

1. Kelly, Thomas C.: Transonic Wind-Tunnel Investigation of the Static Longitudinal Aerodynamic Characteristics of Several Configurations of the Scout Vehicle and of a Number of Related Models. NASA TN D-794, 1961.

2. Pearson, Albin O.: Wind-Tunnel Investigation at Transonic Speeds of the Static Aerodynamic Characteristics and Pressure Distributions of a Three-Stage Saturn Launch Vehicle. NASA TM X-738, 1963.

3. Kelly, Thomas C., and Keynton, Robert J.: Investigation of the Static Longitudinal Aerodynamic Characteristics of a 1/10-Scale Model of the Blue Scout Jr. at Mach Numbers From 0.40 to 1.03. NASA TN D-1228, 1962.

4. Treon, Stuart L.: Effects of Nose-Cone Angle on the Transonic Aerodynamic Characteristics of a Blunt Cone-Cylinder Body Having a Cylindrical, Flared, or Blunt-Finned Afterbody. NASA TM X-582, 1961.

5. Wakefield, Roy M., Treon, Stuart L., and Knechtel, Earl D.: Effects of Centerbody Length and Nose Shape on the Transonic Characteristics of Low-Fineness-Ratio Bodies of Revolution With a Flared Afterbody. NASA TM X-366, 1960.

6. Wakefield, Roy M., Knechtel, Earl D., and Treon, Stuart L.: Transonic Static Aerodynamic Characteristics of a Blunt Cone-Cylinder Body With Flared Afterbodies of Various Angles and Base Areas. NASA TM X-106, 1959.

7. Glover, Warren G.: Investigation of the Aerodynamics of Basic Multistage Missile Shapes at Mach Numbers 1.5 to 5.0. AEDC-TR-61-3 (Contract No. AF 40(600)-800 S/A 24(61-73)), Arnold Eng. Dev. Center, July 1961.

8. Kelly, Thomas C., and Keynton, Robert J.: Transonic Wind-Tunnel Investigation of the Static Aerodynamic Characteristics of Several Configurations of the Blue Scout Launch Vehicle. NASA TN D-1958, 1963.

9. Kelly, Thomas C.: Investigation at Transonic Mach Numbers of the Effects of Configuration Geometry on Surface Pressure Distributions for a Simulated Launch Vehicle. NASA TM X-845, 1963.

10. Treon, Stuart L.: The Effect of Nose Shape on the Static Aerodynamic Characteristics of Ballistic-Type Missile Models at Mach Numbers From 0.6 to 1.4. NASA MEMO 5-17-59A, 1959.

11. Hart, Roger G.: Flight Investigation at Mach Numbers From 0.8 to 1.5 to Determine the Effects of Nose Bluntness on the Total Drag of Two Fin-Stabilized Bodies of Revolution. NACA TN 3549, 1955. (Supersedes NACA RM L50I08a.)

[redacted]

12. Geudtner, W. J., Jr.: Sharp and Blunted Cone Force Coefficients and Centers of Pressure From Wind Tunnel Tests at Mach Numbers From 0.50 to 4.06. Rep. No. ZA-7-017, Convair, June 16, 1955.

[redacted]

[redacted]

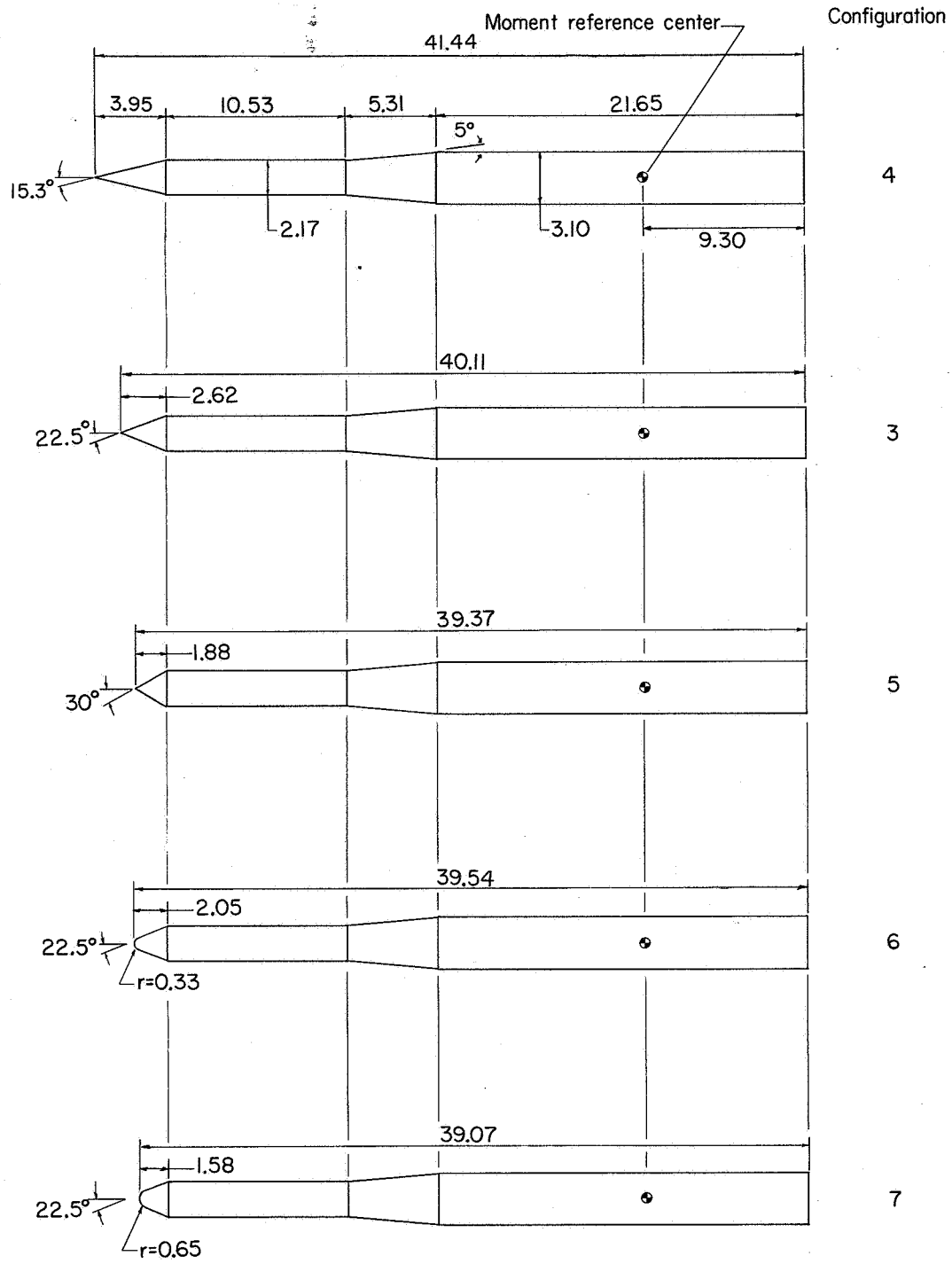

(a) Nose-cone angle and bluntness variations.

Figure 1.- Model details. All dimensions are in inches unless otherwise noted.

[redacted]

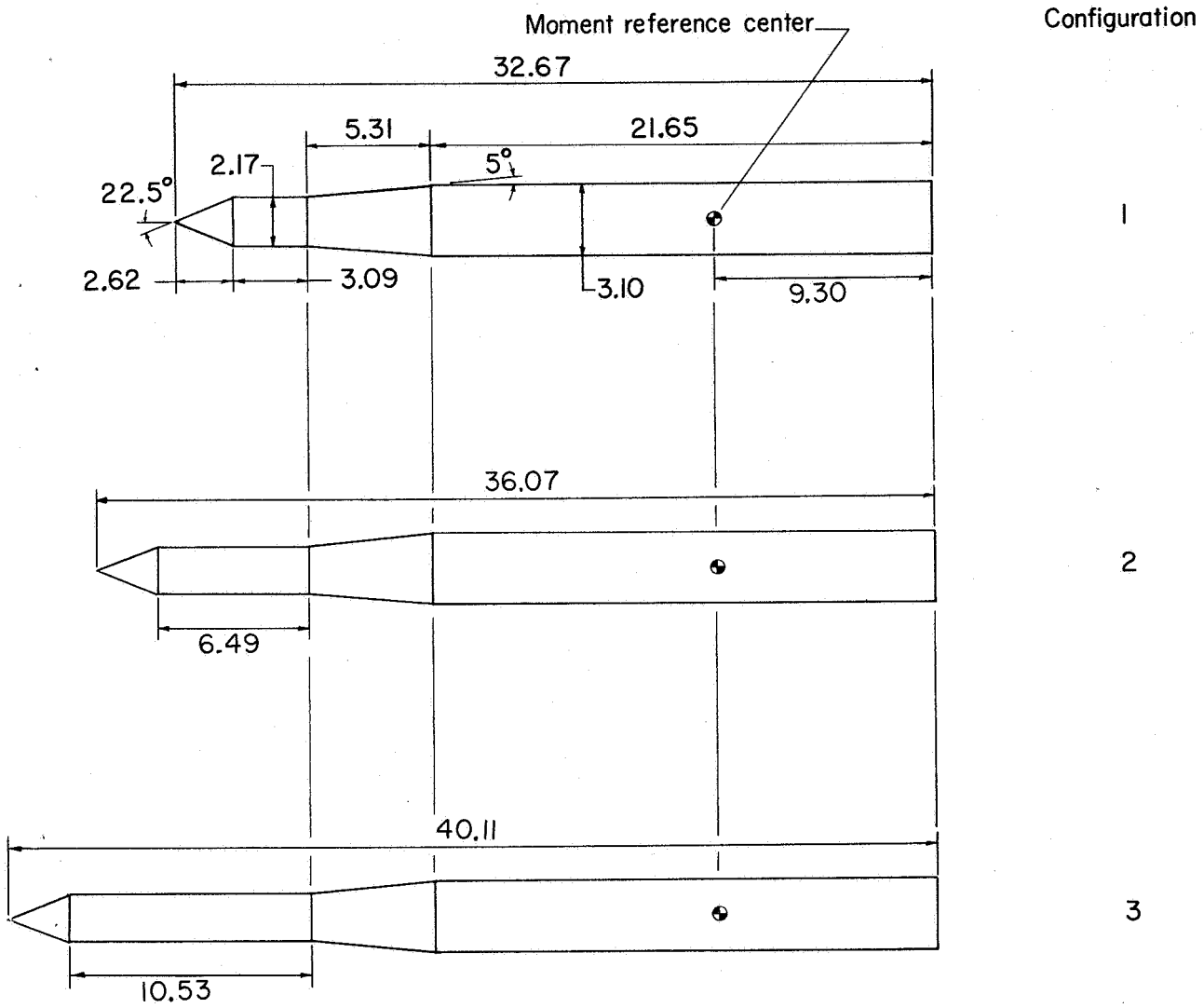

(b) Upper-stage fineness-ratio variations.

Figure 1.- Continued.

[redacted]

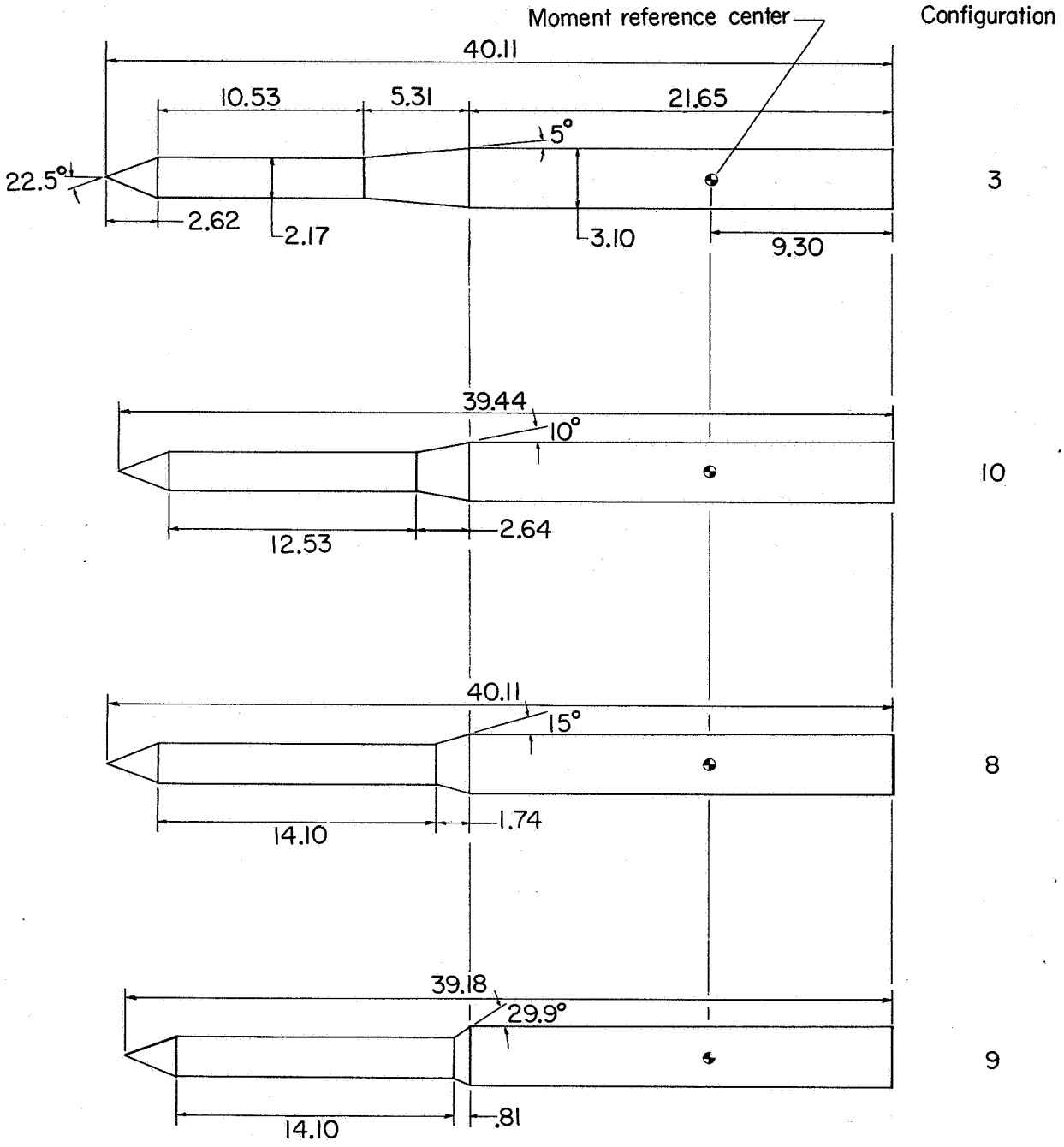

(c) Transition flare angle variations.

Figure 1.- Concluded.

[redacted]

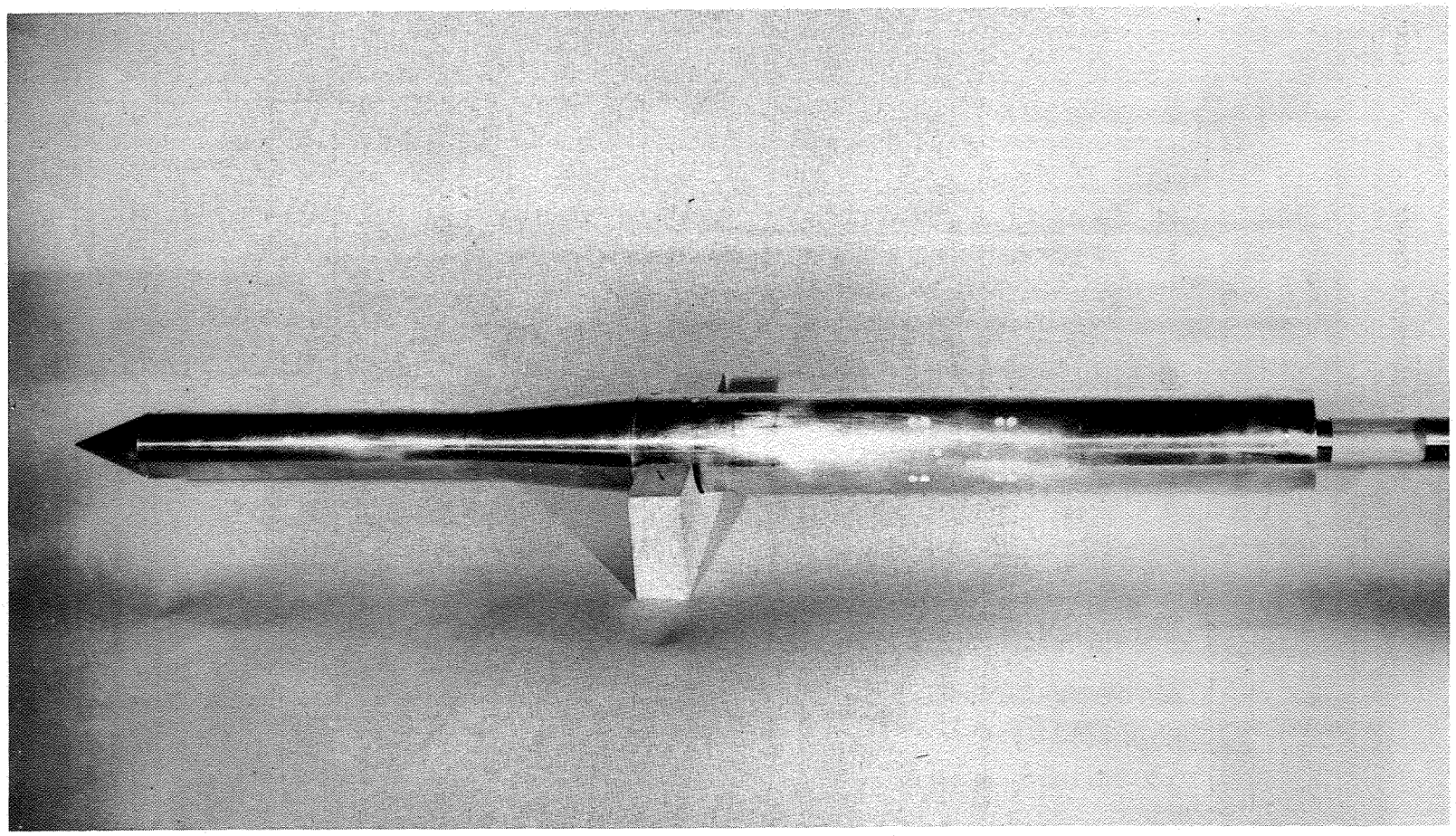

(a) Typical arrangement, configuration 3.

L-63-5586

Figure 2.- Model photographs.

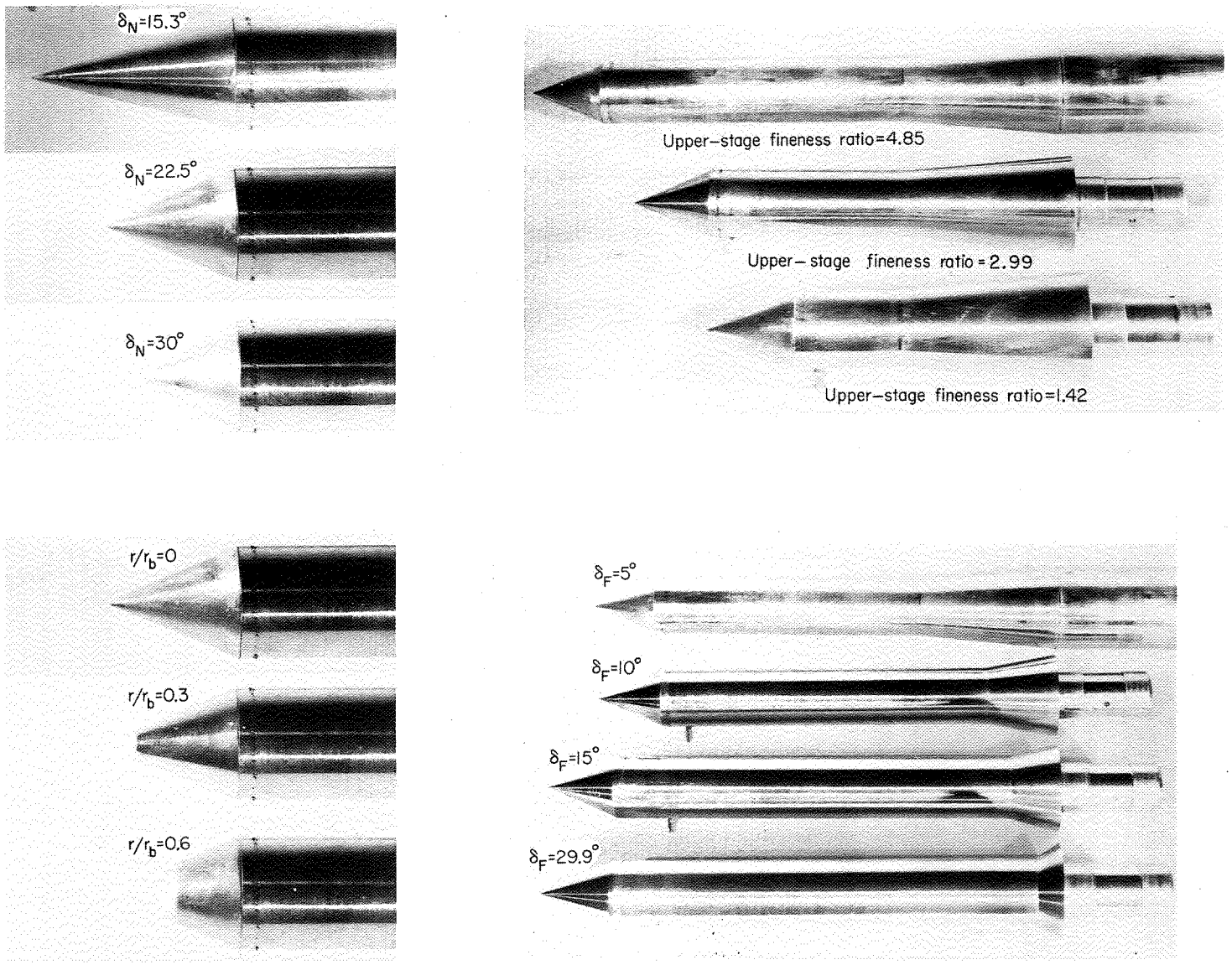

(b) Nose, upper-stage, and transition flare components. L-64-420

Figure 2.- Concluded.

[redacted]

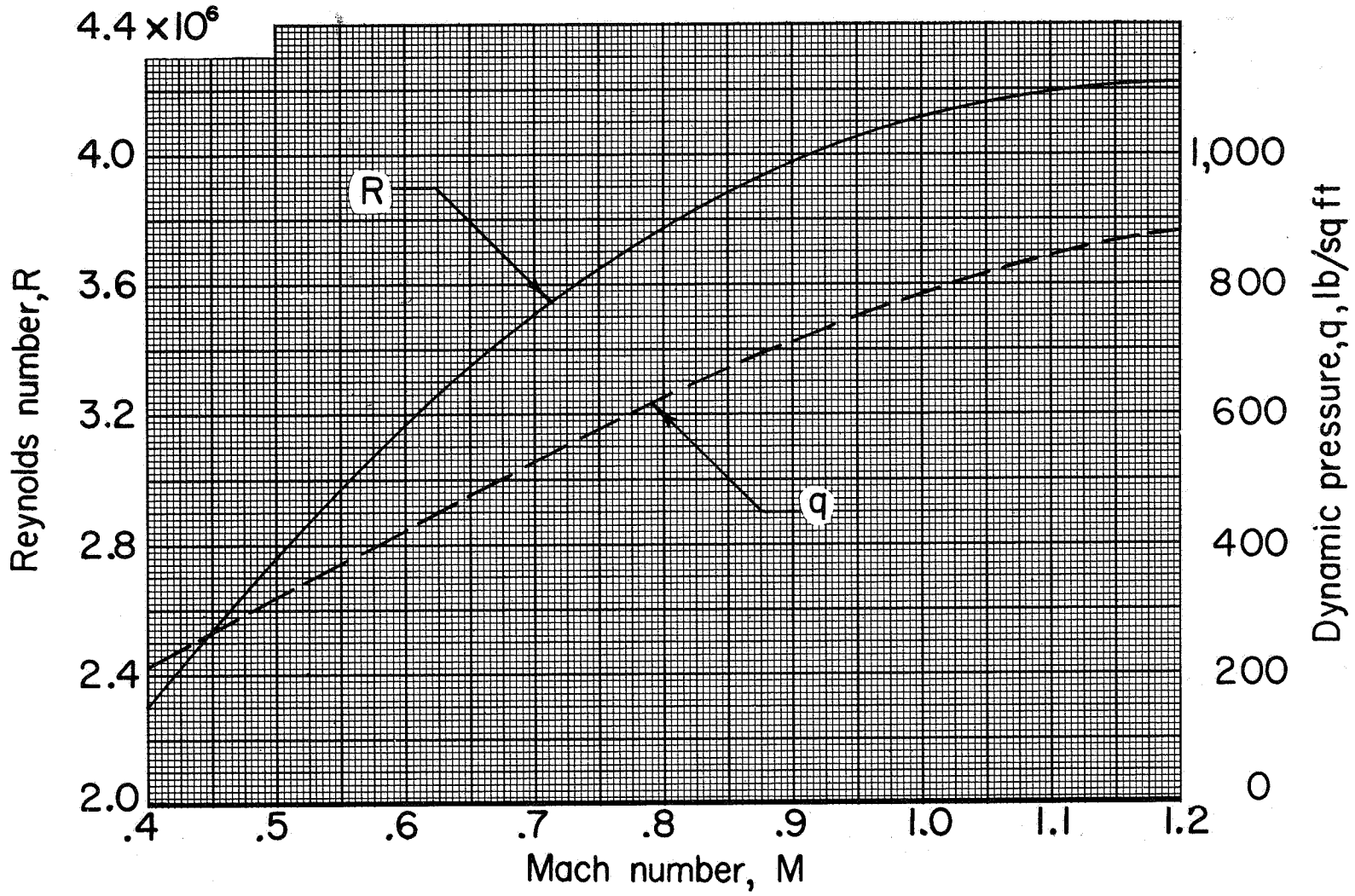

Figure 3.- Variation with Mach number of average test Reynolds number per foot and dynamic pressure.

[redacted]

[redacted]

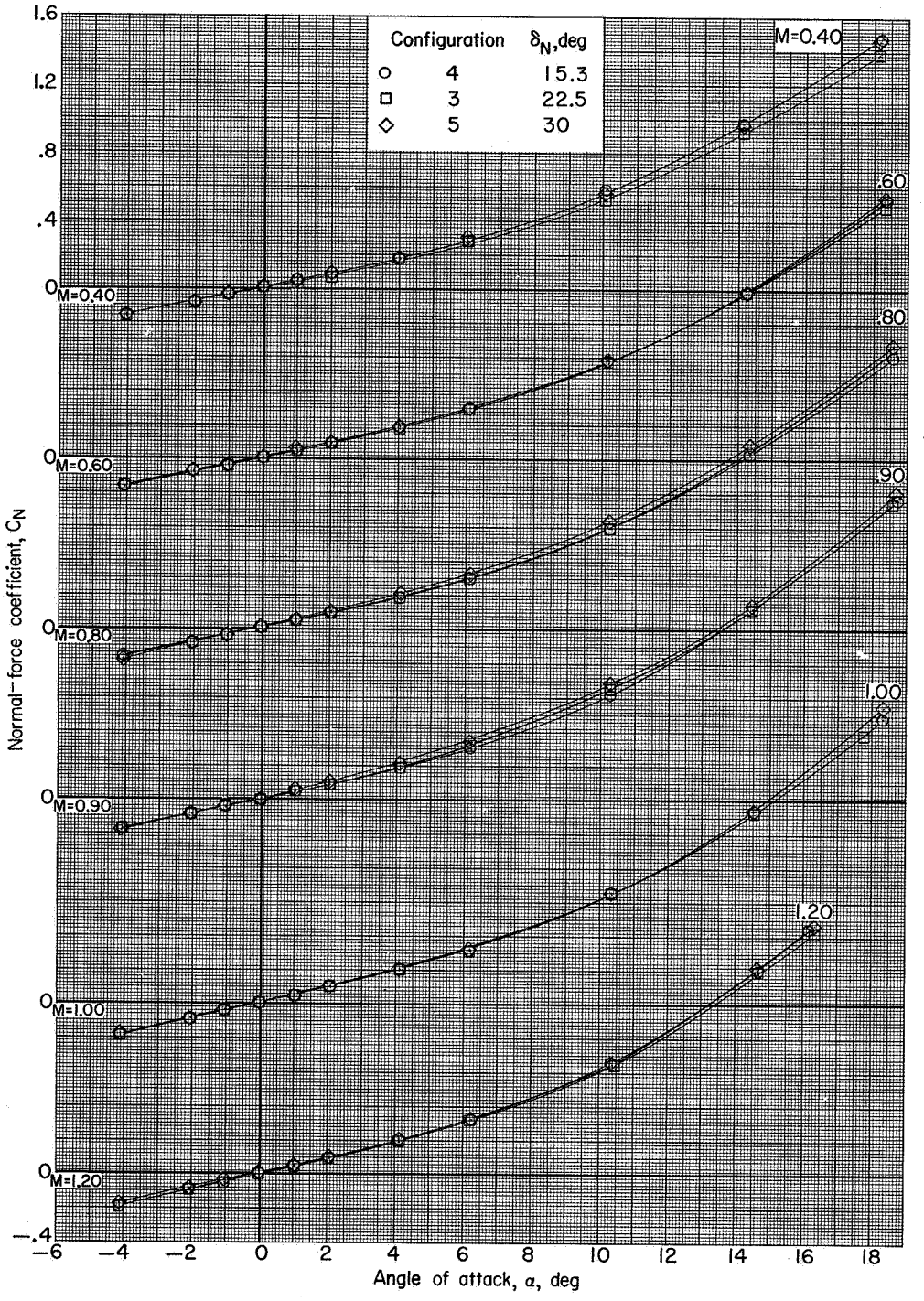

(a) Nose-cone-angle variations.

Figure 4.- Variation with angle of attack of normal-force characteristics.

[redacted]

[redacted]

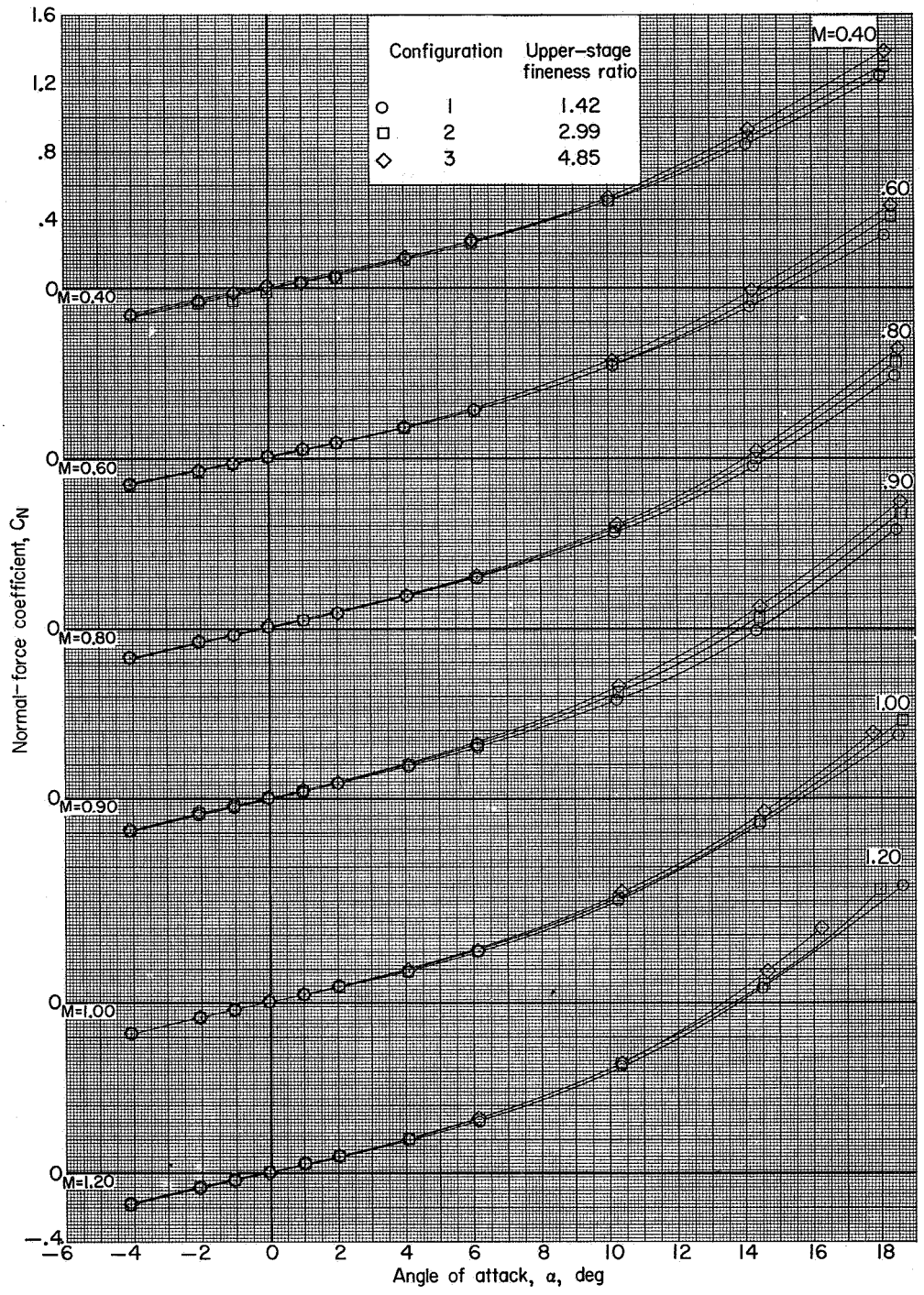

(b) Upper-stage fineness-ratio variations.

Figure 4.- Continued.

[redacted]

[redacted]

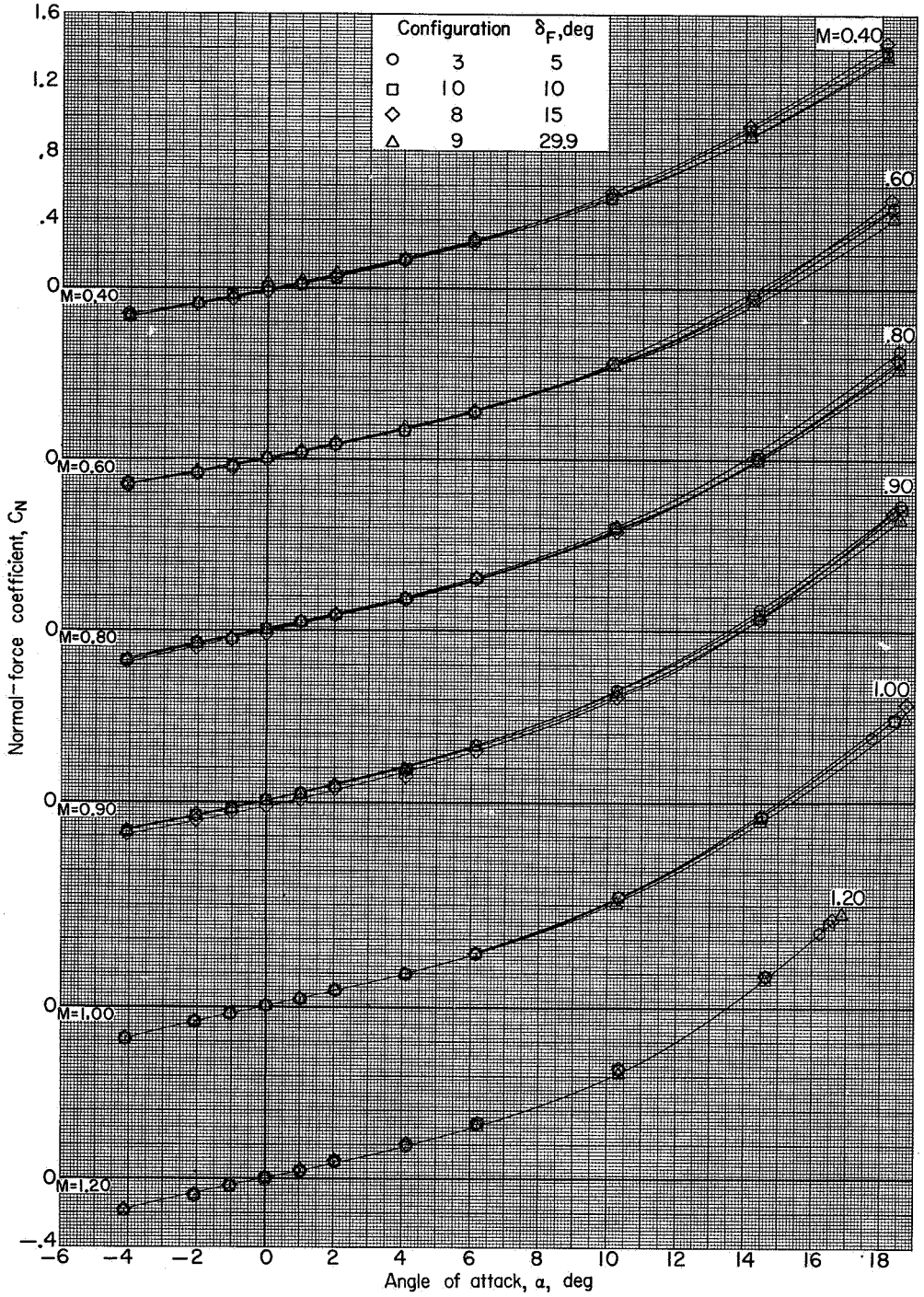

(c) Transition flare angle variations.

Figure 4.- Concluded.

[redacted]

[redacted]

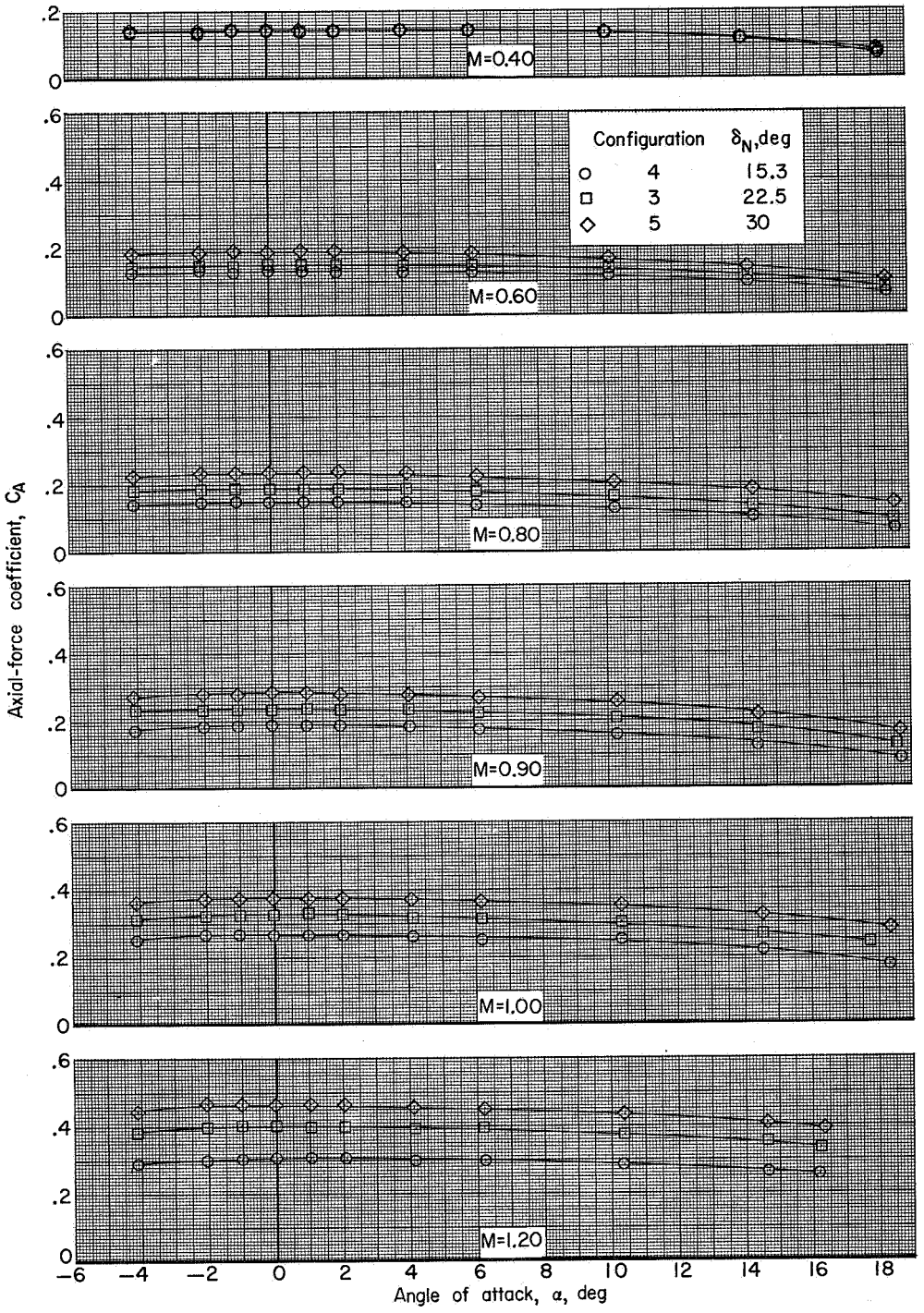

(a) Nose-cone-angle variations.

Figure 5.- Variation with angle of attack of axial-force characteristics.

[redacted]

[redacted]

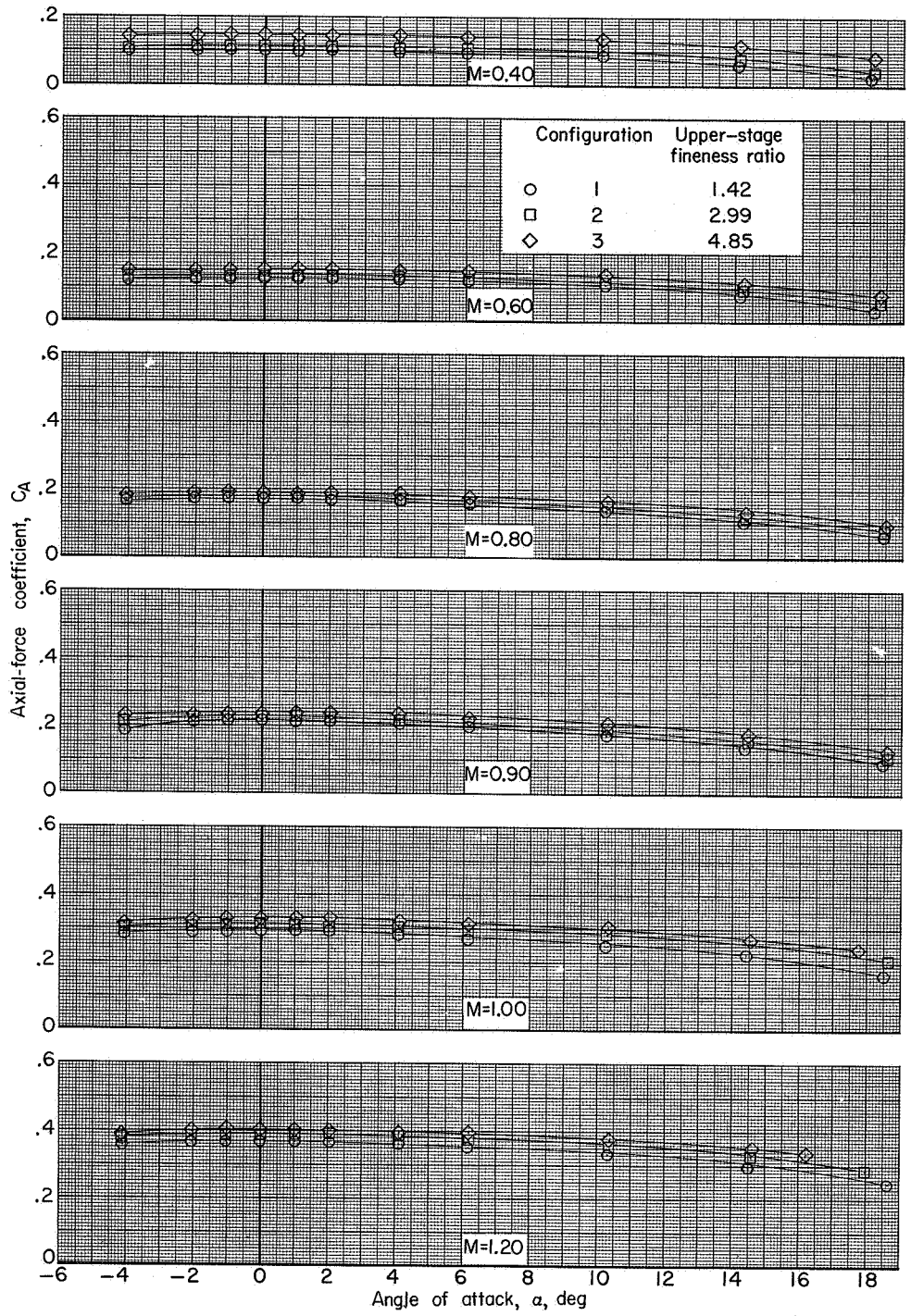

(b) Upper-stage fineness-ratio variations.

Figure 5.- Continued.

[redacted]

[redacted]

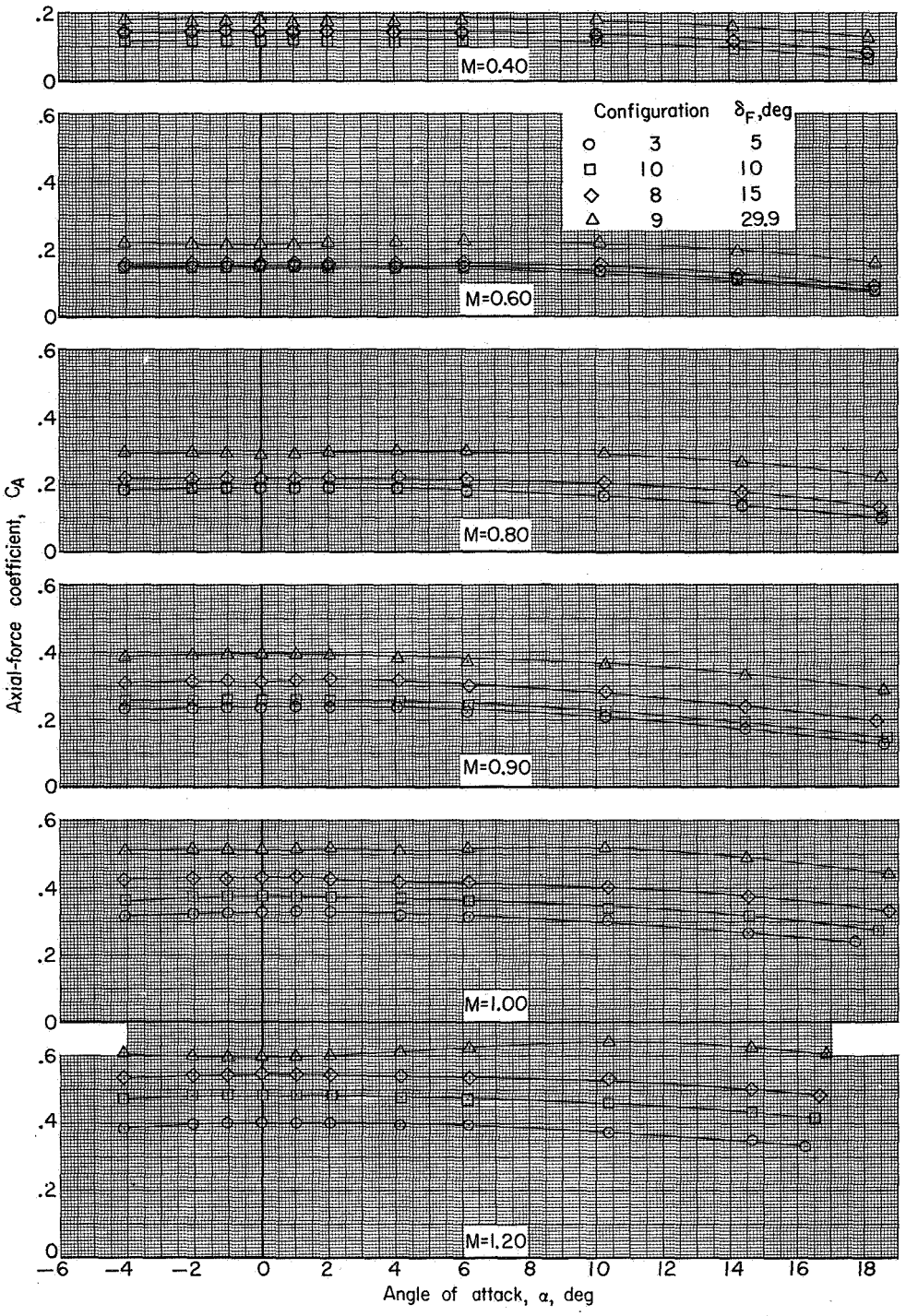

(c) Transition flare angle variations.

Figure 5.- Concluded.

[redacted]

[redacted]

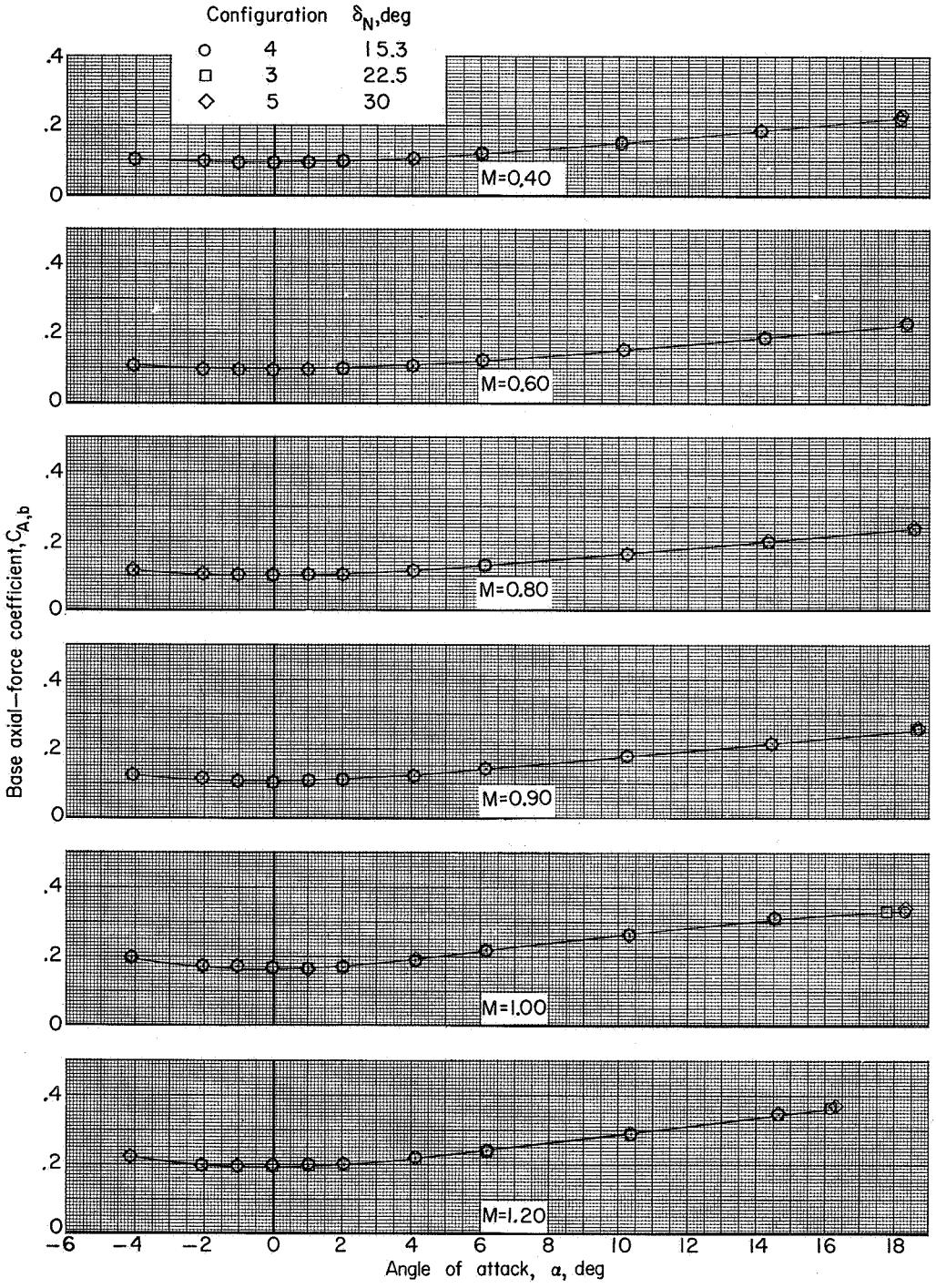

(a) Nose-cone-angle variations.

Figure 6.- Variation with angle of attack of base axial-force characteristics.

[redacted]

[redacted]

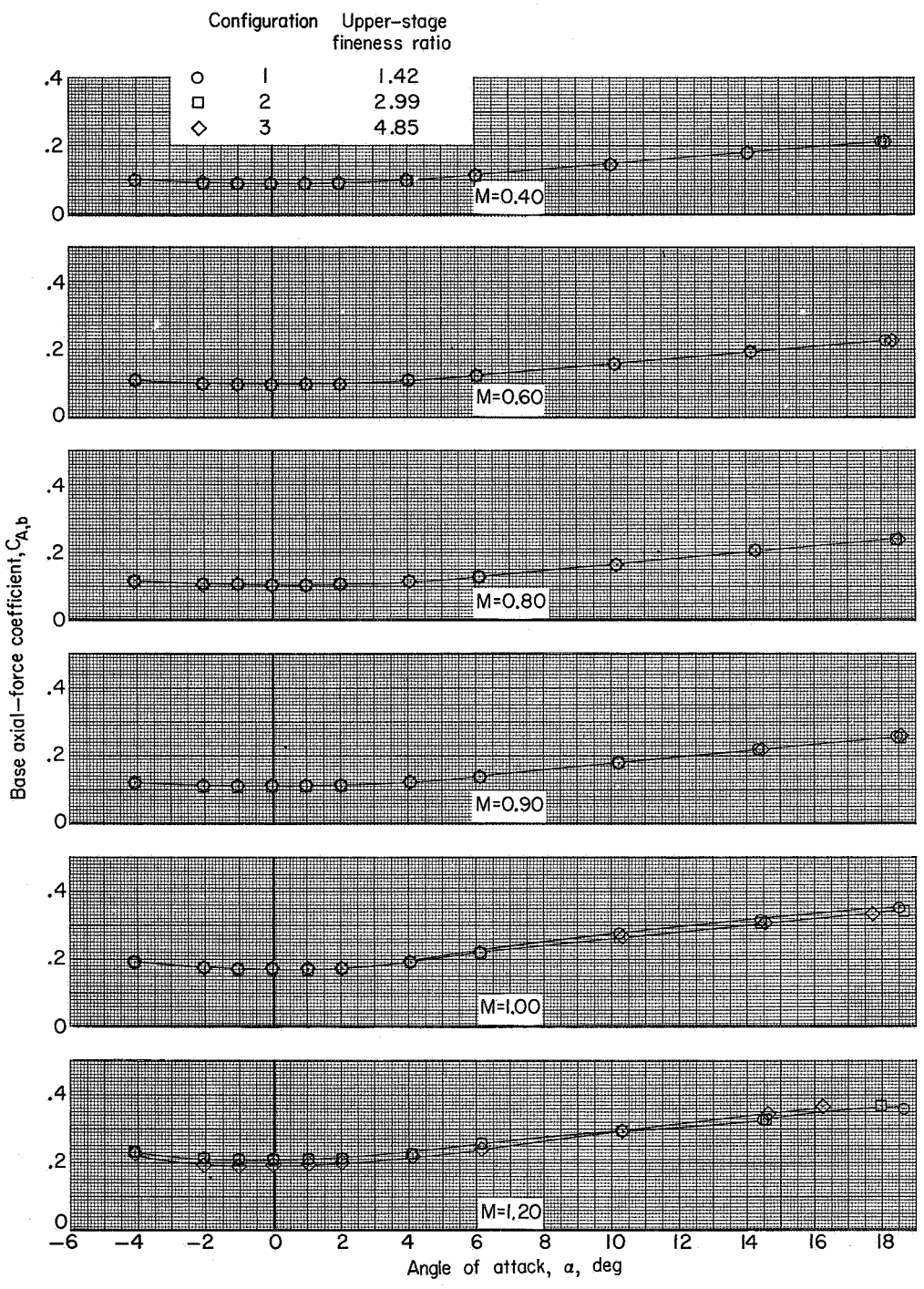

(b) Upper-stage fineness-ratio variations.

Figure 6.- Continued.

[redacted]

[redacted]

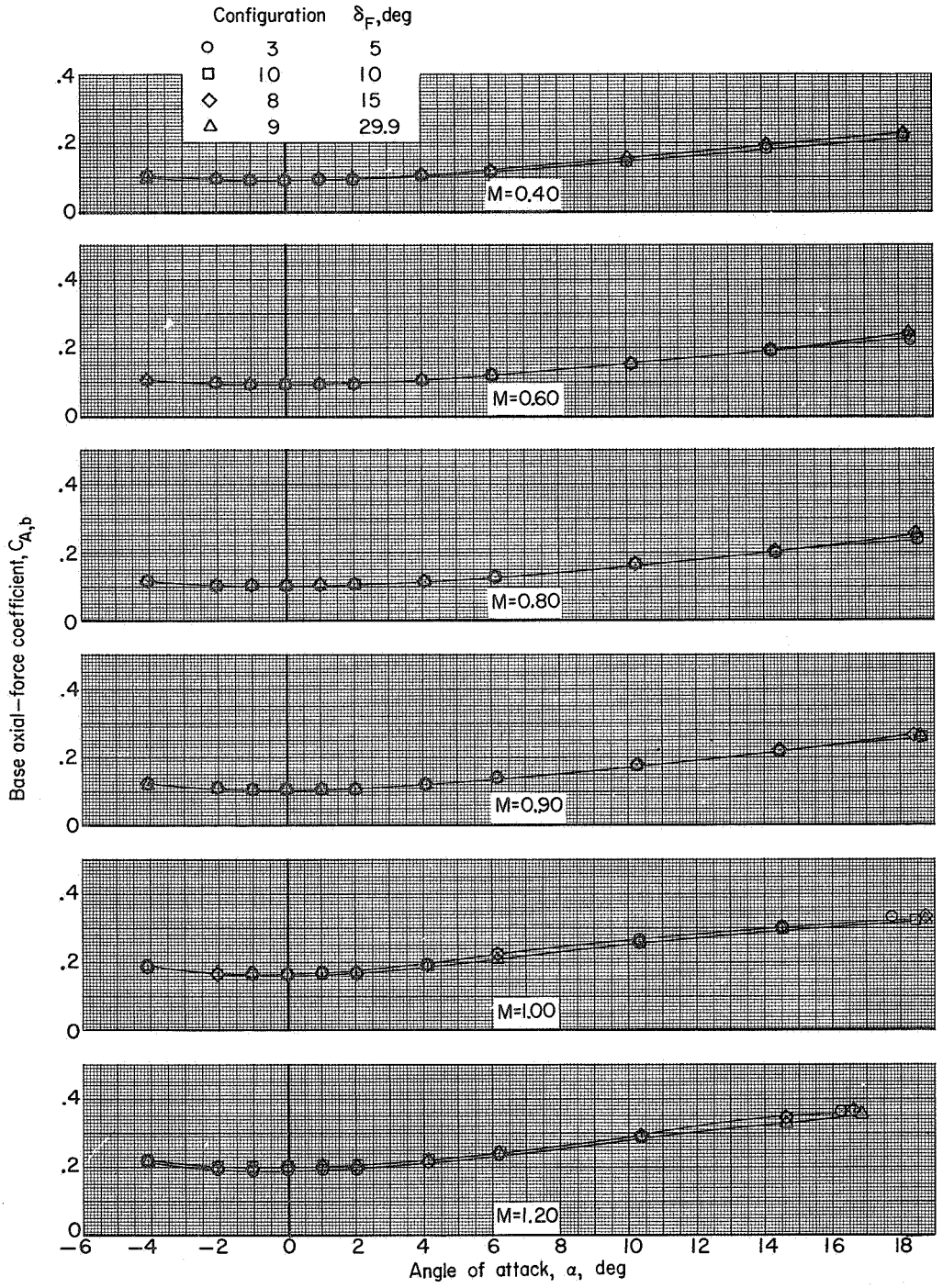

(c) Transition flare angle variations.

Figure 6.- Concluded.

[redacted]

[redacted]

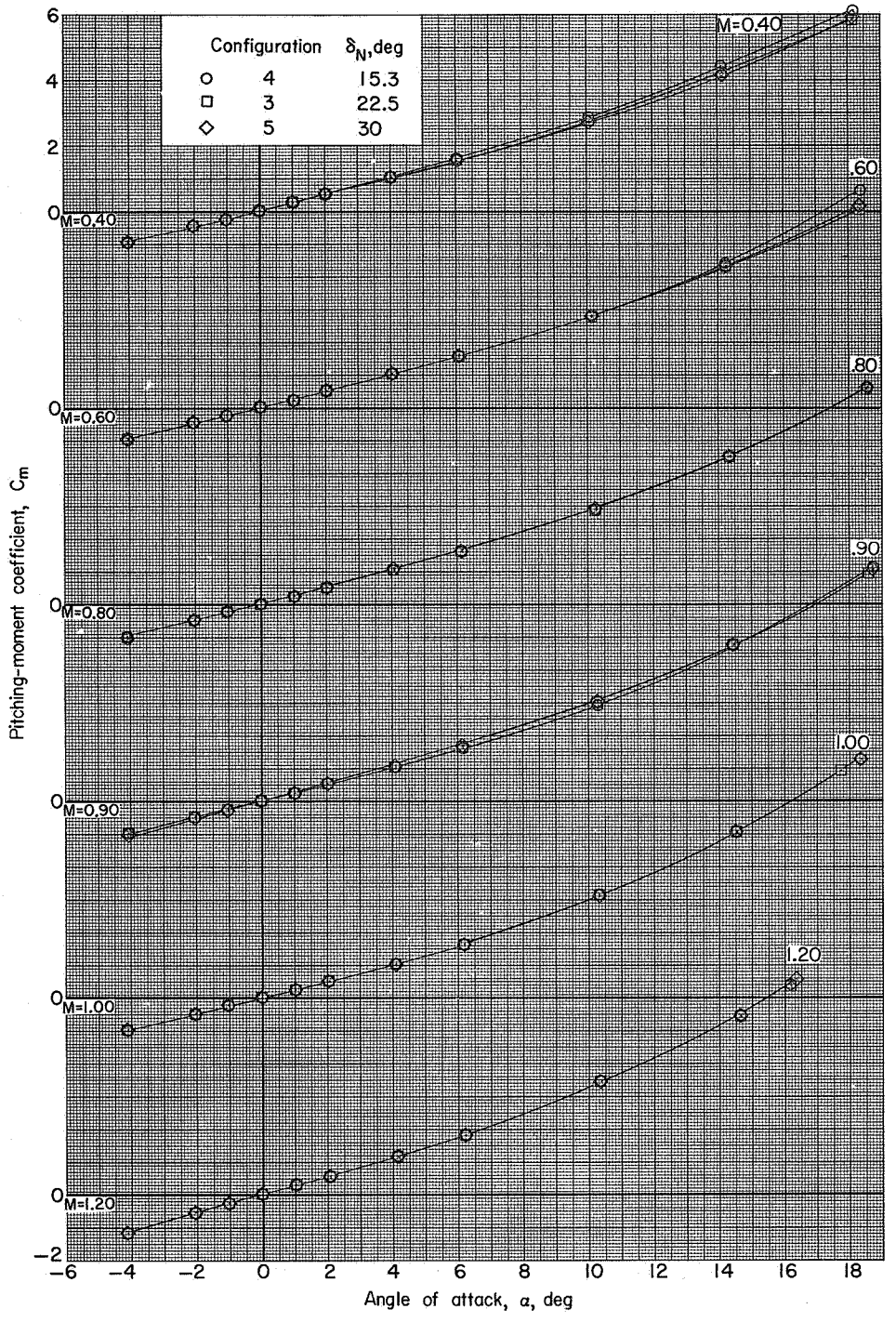

(a) Nose-cone-angle variations.

Figure 7.- Variation with angle of attack of pitching-moment characteristics.

[redacted]

[redacted]

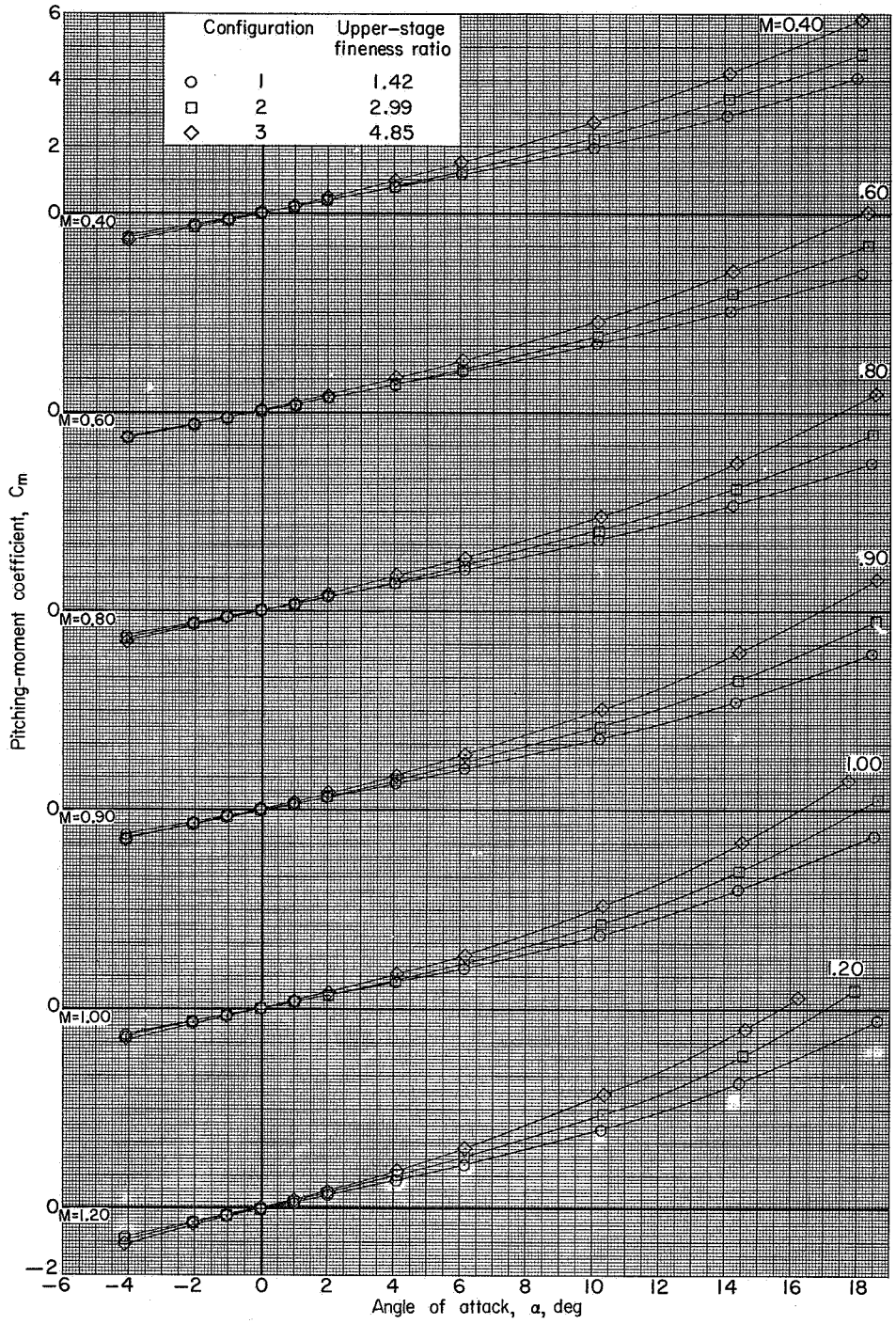

(b) Upper-stage fineness-ratio variations.

Figure 7.- Continued.

[redacted]

[redacted]

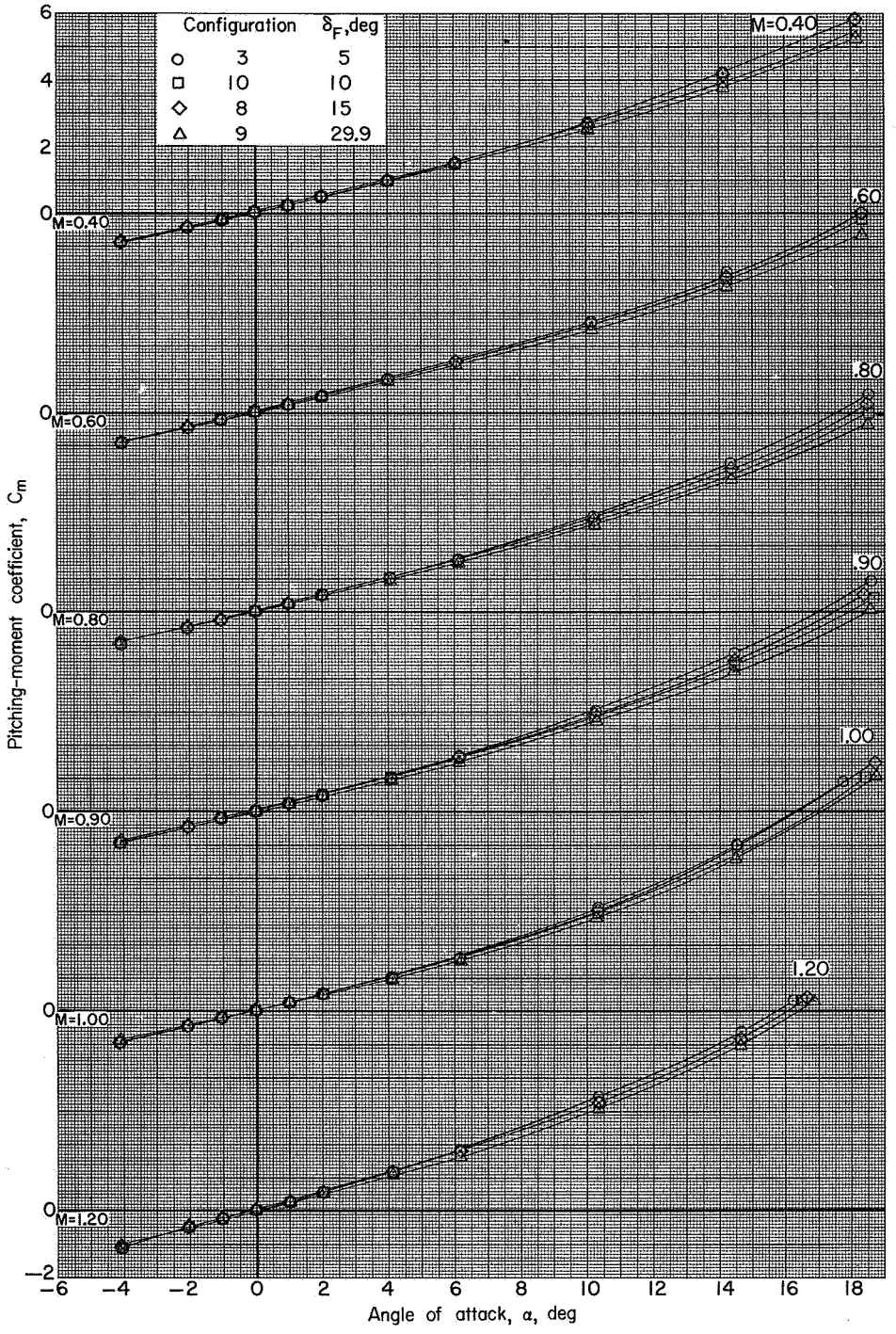

(c) Transition flare angle variations.

Figure 7.- Concluded.

[redacted]

[redacted]

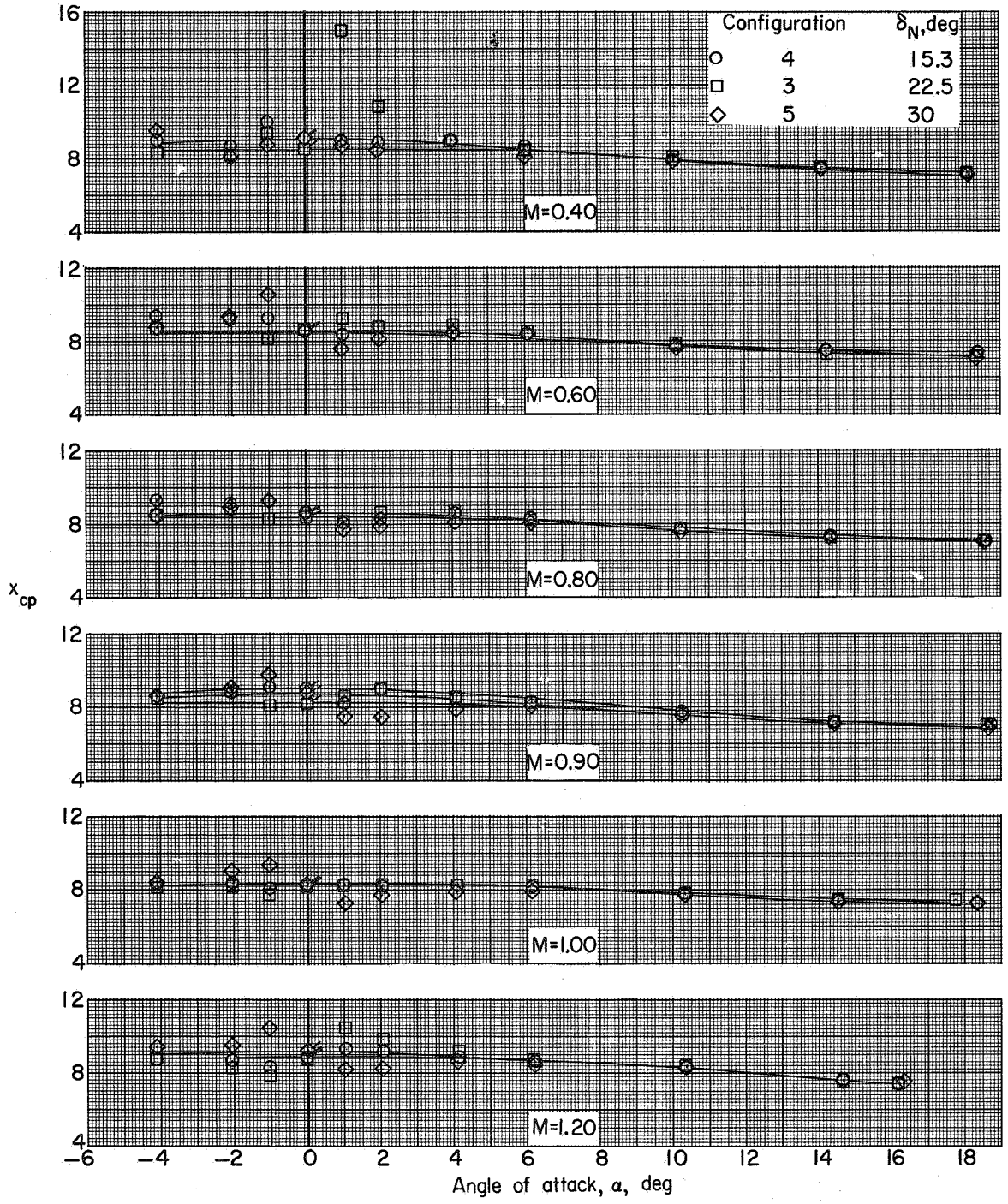

(a) Nose-cone-angle variations.

Figure 8.- Variation with angle of attack of center-of-pressure characteristics.

[redacted]

[redacted]

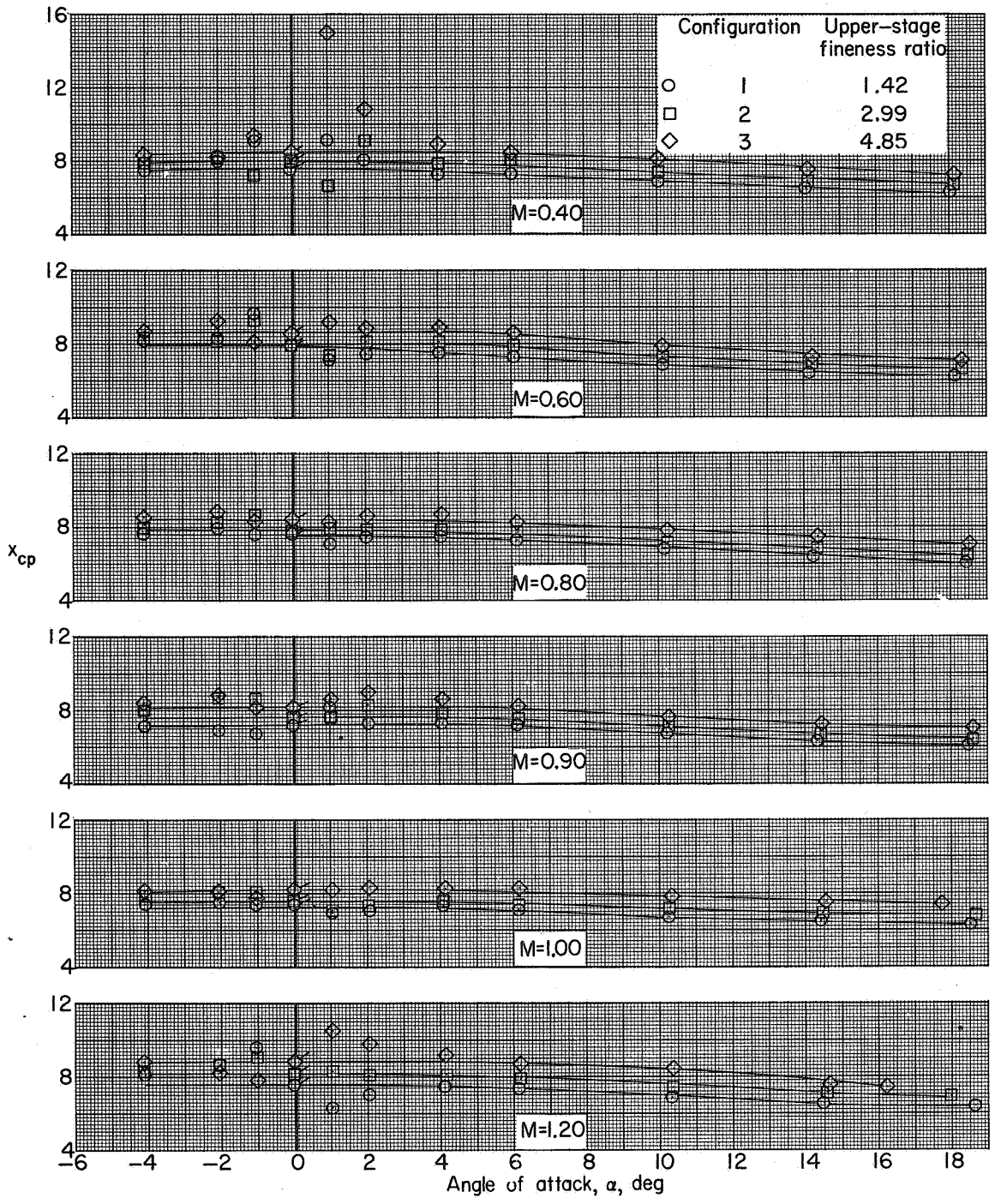

(b) Upper-stage fineness-ratio variations.

Figure 8.- Continued.

[redacted]

[redacted]

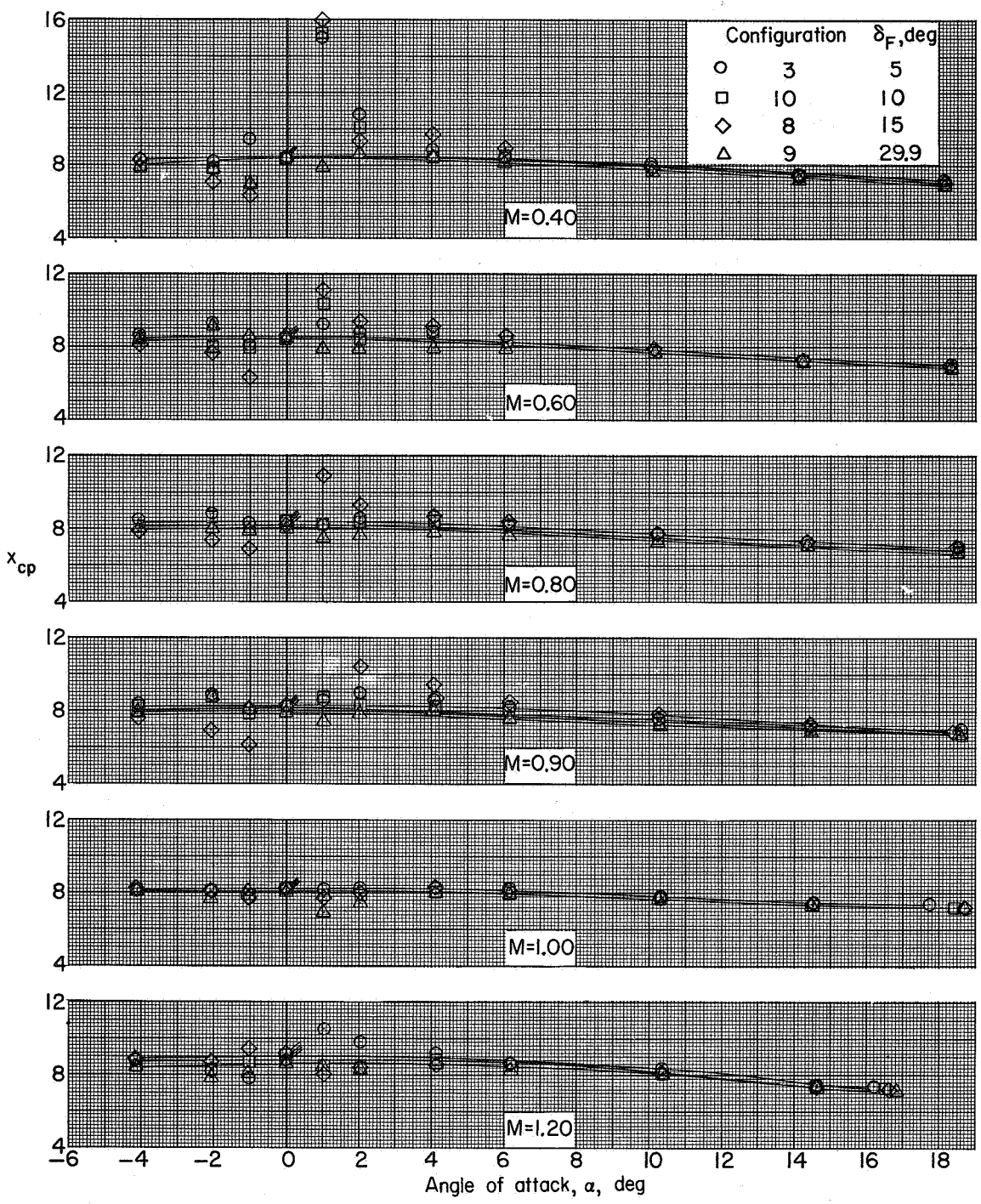

(c) Transition flare angle variations.

Figure 8.- Concluded.

[redacted]

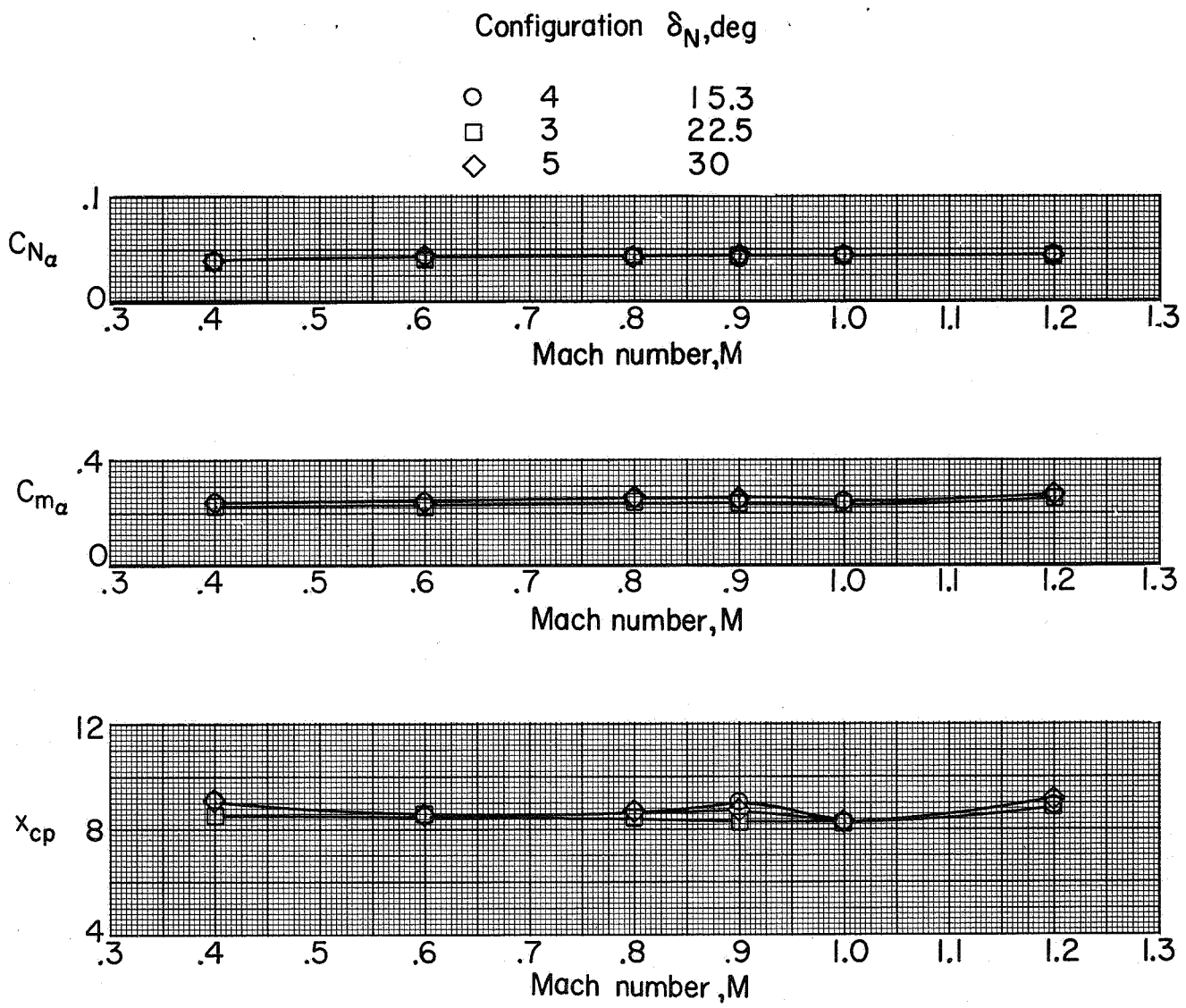

(a) Effect of nose-cone angle.

Figure 9.- Summary of aerodynamic characteristics in pitch. $\alpha \approx 0^{\circ}$.

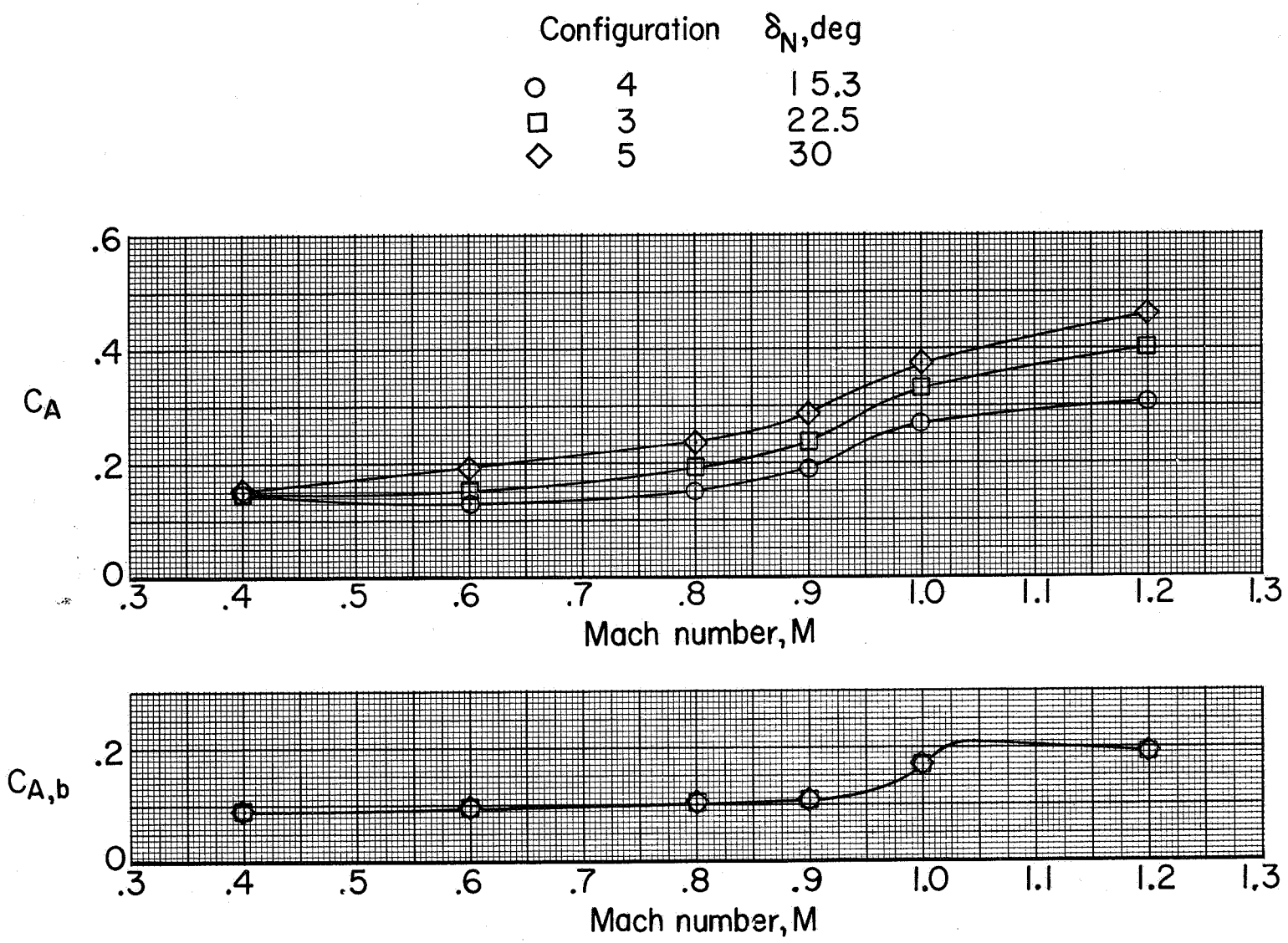

(a) Concluded.

Figure 9.- Continued.

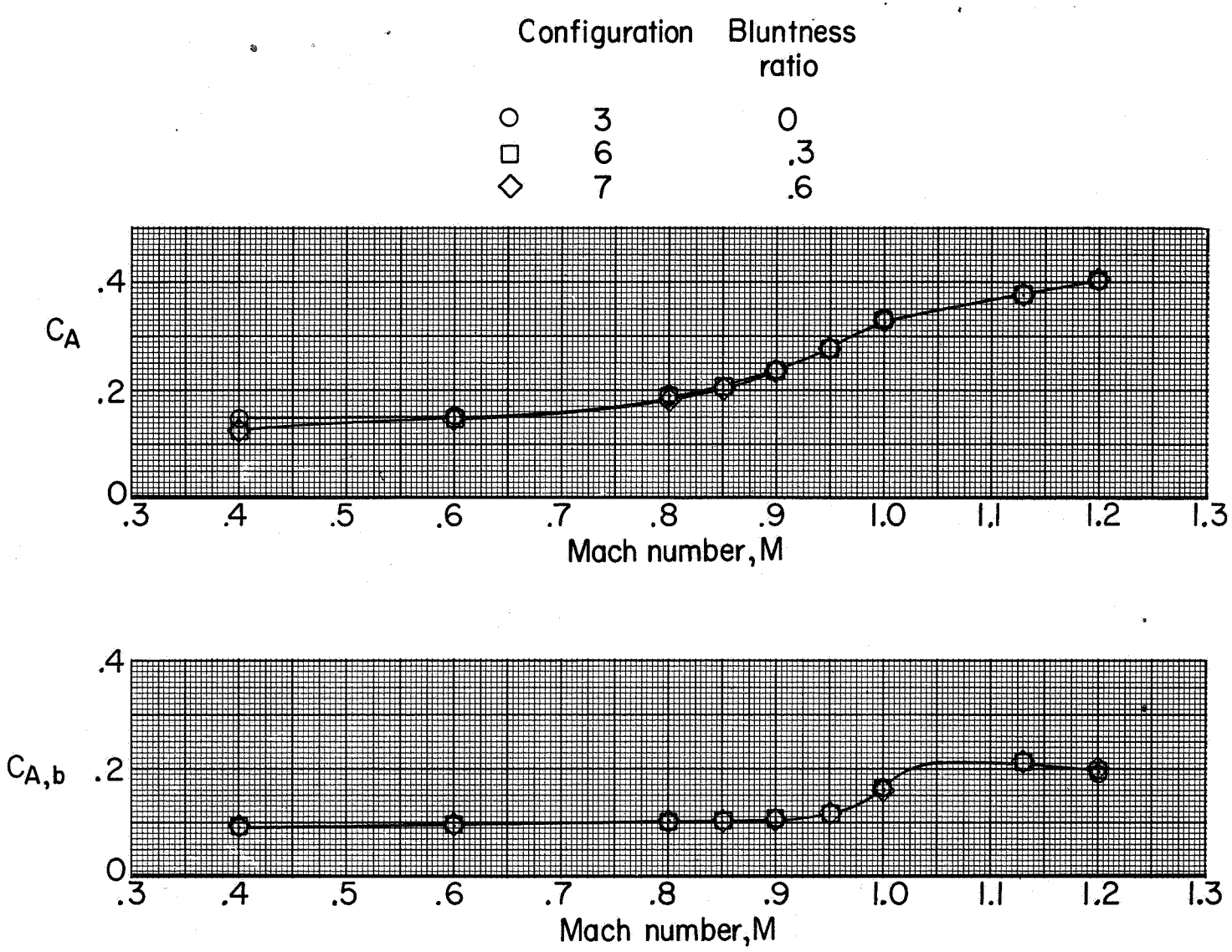

(b) Effect of nose bluntness.

Figure 9.- Continued.

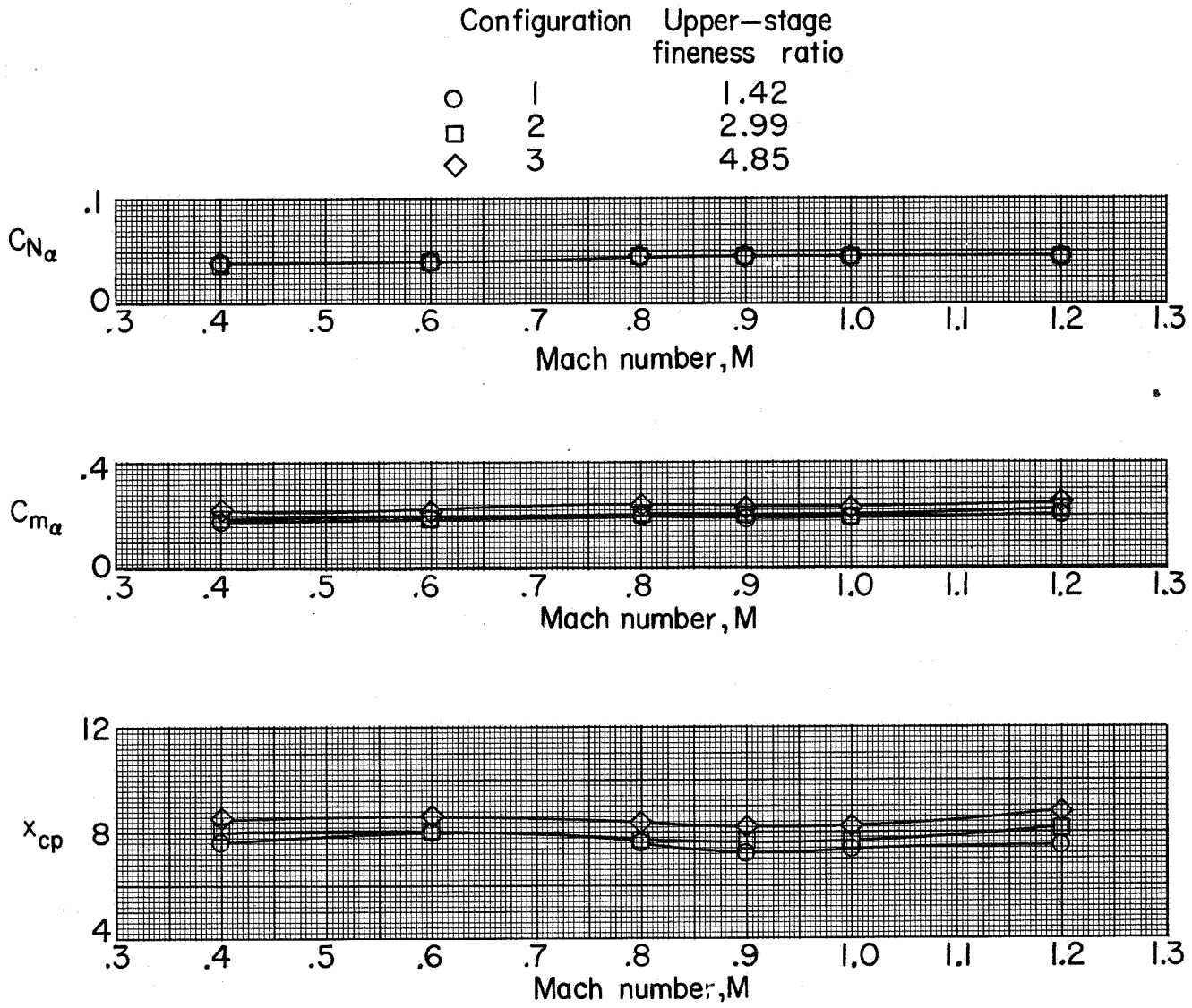

(c) Effect of upper-stage fineness ratio.

Figure 9.- Continued.

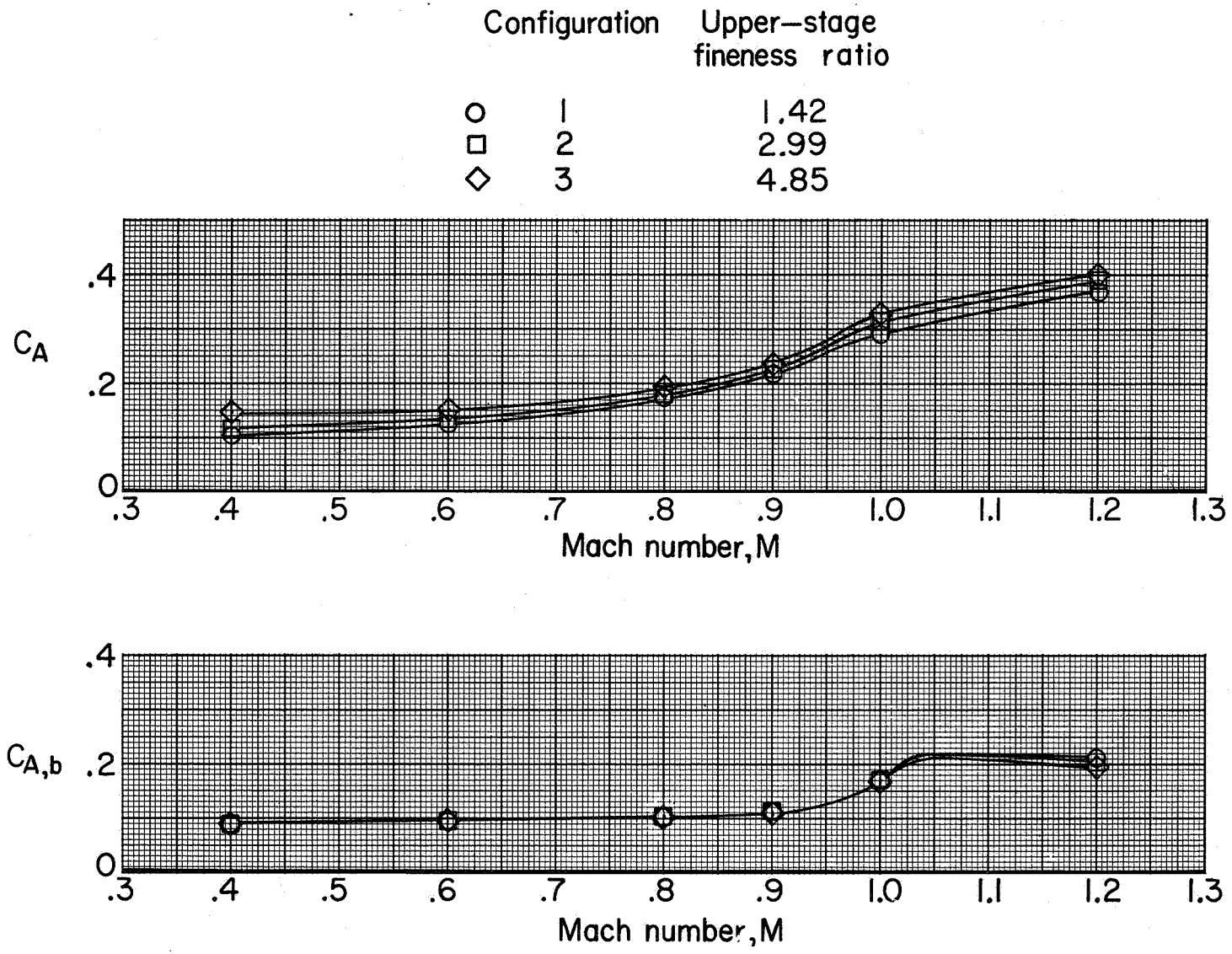

(c) Concluded.

Figure 9.- Continued.

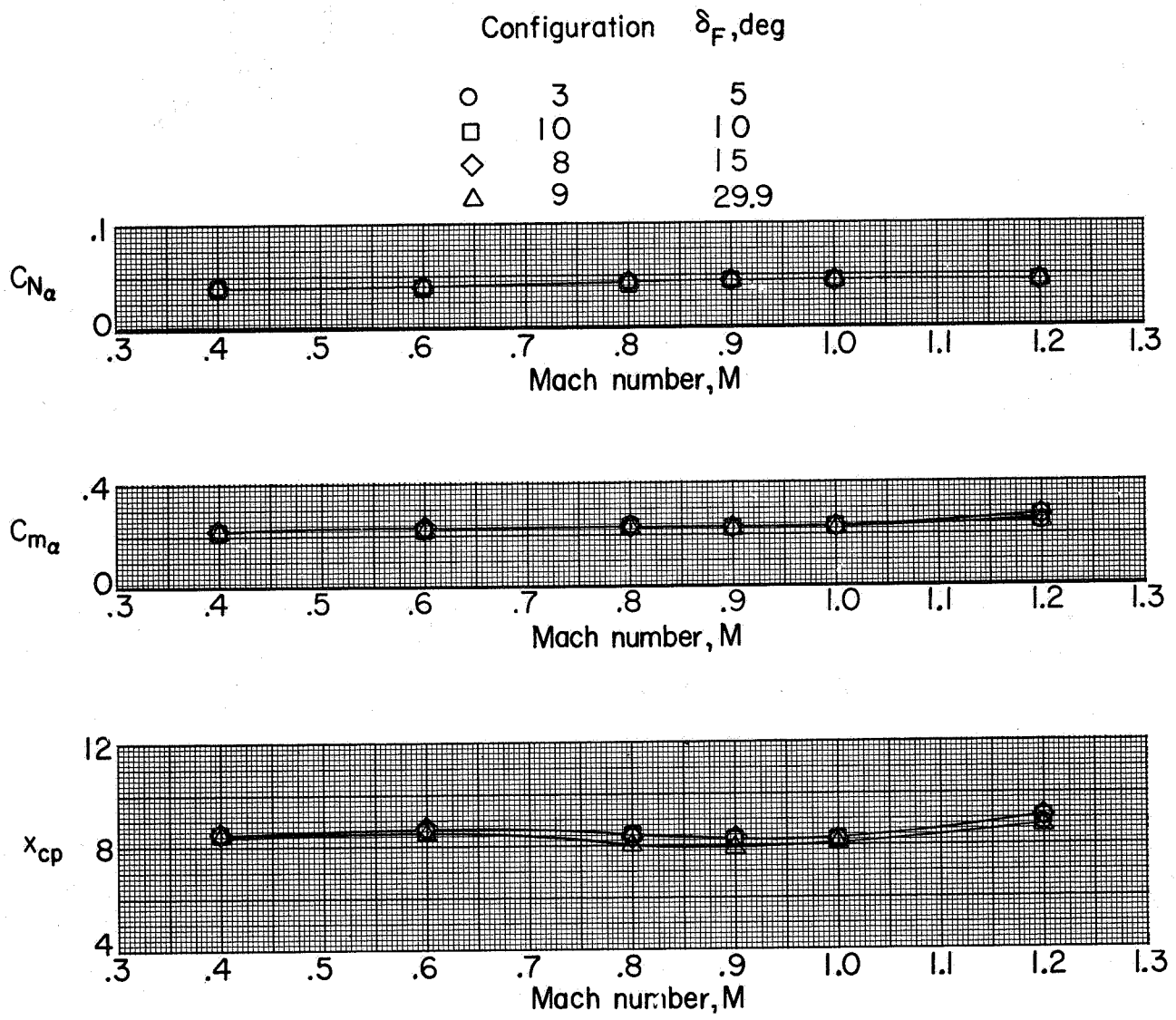

(d) Effect of transition flare angle.

Figure 9.- Continued.

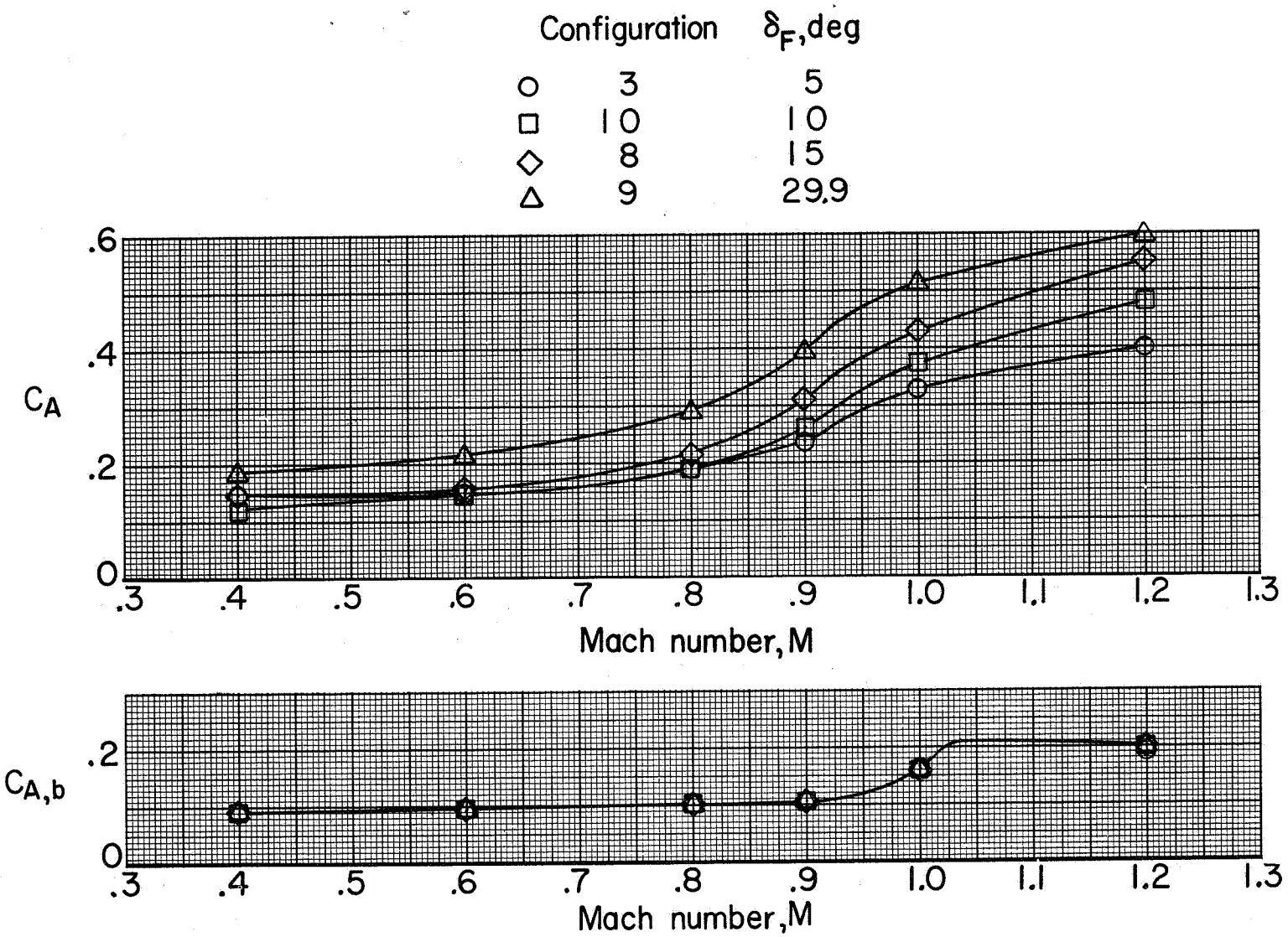

(d) Concluded.

Figure 9.- Concluded.

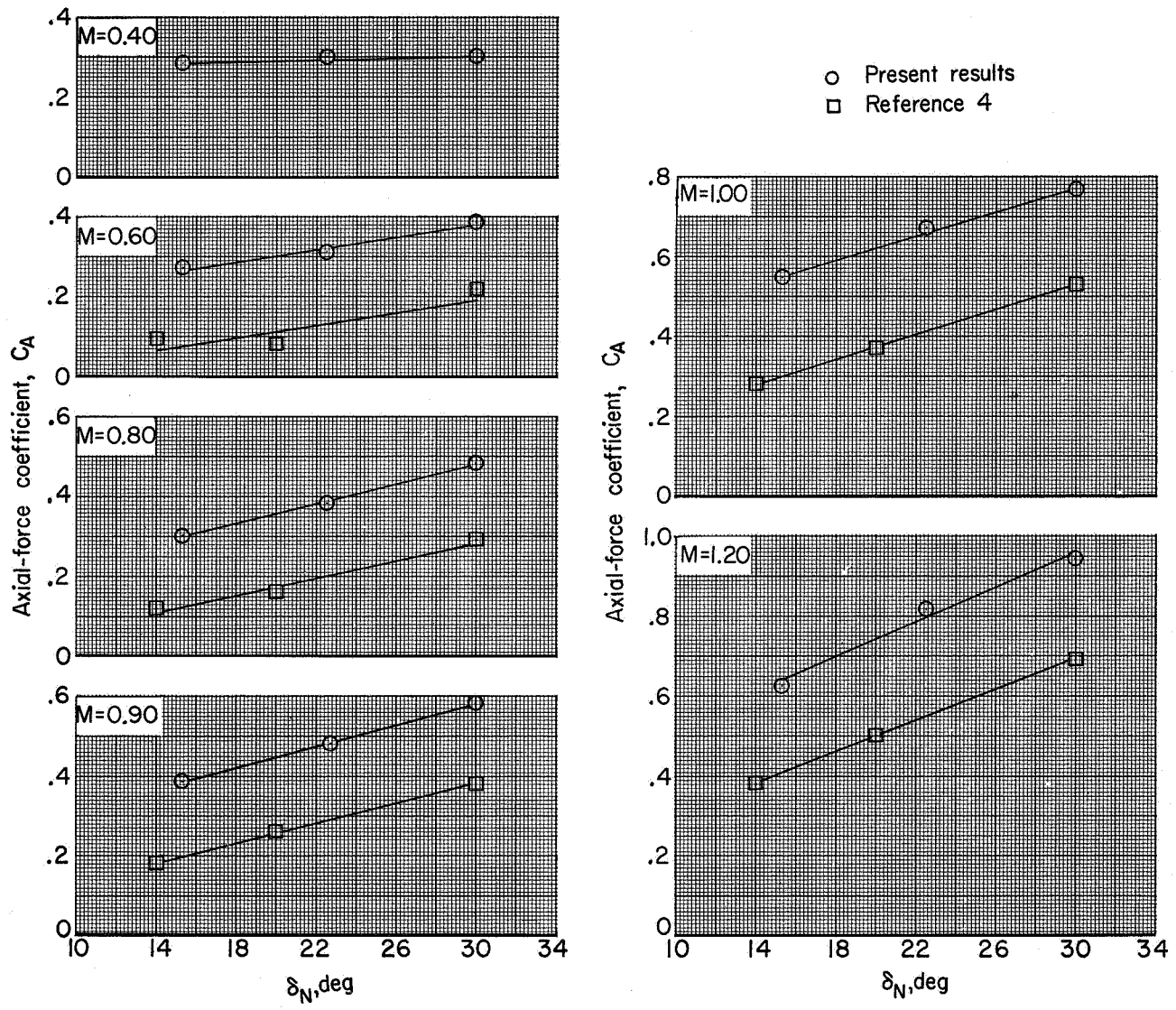

(a) C_A against δ_N.

Figure 10.- Effect of nose-cone angle on axial-force characteristics.

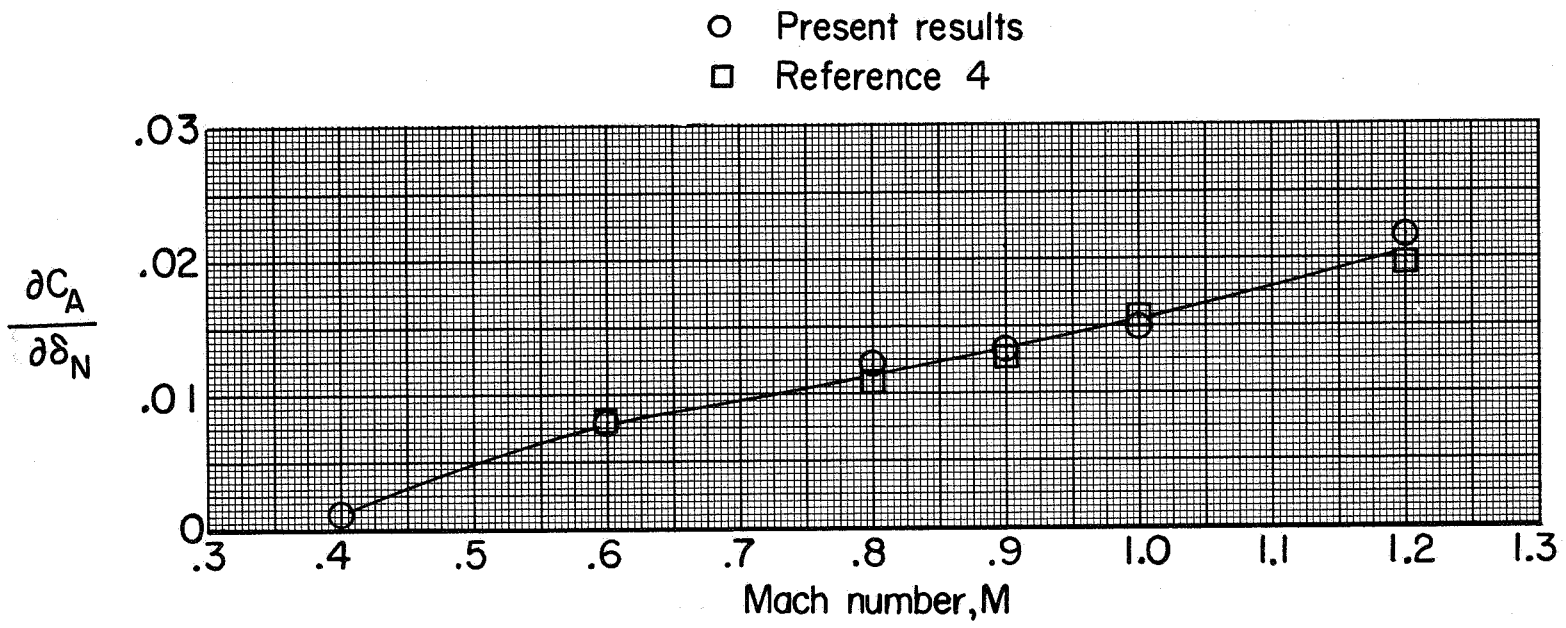

(b) $\partial C_A/\partial \delta_N$ against M.

Figure 10.- Concluded.

[redacted]

"The aeronautical and space activities of the United States shall be conducted so as to contribute . . . to the expansion of human knowledge of phenomena in the atmosphere and space. The Administration shall provide for the widest practicable and appropriate dissemination of information concerning its activities and the results thereof."

—NATIONAL AERONAUTICS AND SPACE ACT OF 1958

NASA SCIENTIFIC AND TECHNICAL PUBLICATIONS

TECHNICAL REPORTS: Scientific and technical information considered important, complete, and a lasting contribution to existing knowledge.

TECHNICAL NOTES: Information less broad in scope but nevertheless of importance as a contribution to existing knowledge.

TECHNICAL MEMORANDUMS: Information receiving limited distribution because of preliminary data, security classification, or other reasons.

CONTRACTOR REPORTS: Technical information generated in connection with a NASA contract or grant and released under NASA auspices.

TECHNICAL TRANSLATIONS: Information published in a foreign language considered to merit NASA distribution in English.

TECHNICAL REPRINTS: Information derived from NASA activities and initially published in the form of journal articles.

SPECIAL PUBLICATIONS: Information derived from or of value to NASA activities but not necessarily reporting the results of individual NASA-programmed scientific efforts. Publications include conference proceedings, monographs, data compilations, handbooks, sourcebooks, and special bibliographies.

Details on the availability of these publications may be obtained from:

SCIENTIFIC AND TECHNICAL INFORMATION DIVISION

NATIONAL AERONAUTICS AND SPACE ADMINISTRATION

Washington, D.C. 20546

[redacted]